ORIGINAL ARTICLE

Journal of Anatomy   ANATOMICAL SOCIETY WILEY

The vomeronasal system of the wolf (*Canis lupus signatus*): The singularities of a wild canid

Irene Ortiz-Leal[1] | Mateo V. Torres[1] | José-Daniel Barreiro-Vázquez[1] | Ana López-Beceiro[1] | Luis Fidalgo[1] | Taekyun Shin[2] | Pablo Sanchez-Quinteiro[1]

[1]Department of Anatomy, Animal Production and Clinical Veterinary Sciences, Faculty of Veterinary, University of Santiago de Compostela, Lugo, Spain

[2]College of Veterinary Medicine and Veterinary Medical Research Institute, Jeju National University, Jeju, Republic of Korea

Correspondence
Pablo Sanchez-Quinteiro, Department of Anatomy, Animal Production, and Clinical Veterinary Sciences, Faculty of Veterinary, University of Santiago de Compostela, Av Carballo Calero s/n, 27002 Lugo, Spain.
Email: pablo.sanchez@usc.es

Abstract

Wolves, akin to their fellow canids, extensively employ chemical signals for various aspects of communication, including territory maintenance, reproductive synchronisation and social hierarchy signalling. Pheromone-mediated chemical communication operates unconsciously among individuals, serving as an innate sensory modality that regulates both their physiology and behaviour. Despite its crucial role in the life of the wolf, there is a lacuna in comprehensive research on the neuroanatomical and physiological underpinnings of chemical communication within this species. This study investigates the vomeronasal system (VNS) of the Iberian wolf, simultaneously probing potential alterations brought about by dog domestication. Our findings demonstrate the presence of a fully functional VNS, vital for pheromone-mediated communication, in the Iberian wolf. While macroscopic similarities between the VNS of the wolf and the domestic dog are discernible, notable microscopic differences emerge. These distinctions include the presence of neuronal clusters associated with the sensory epithelium of the vomeronasal organ (VNO) and a heightened degree of differentiation of the accessory olfactory bulb (AOB). Immunohistochemical analyses reveal the expression of the two primary families of vomeronasal receptors (V1R and V2R) within the VNO. However, only the V1R family is expressed in the AOB. These findings not only yield profound insights into the VNS of the wolf but also hint at how domestication might have altered neural configurations that underpin species-specific behaviours. This understanding holds implications for the development of innovative strategies, such as the application of semiochemicals for wolf population management, aligning with contemporary conservation goals.

KEYWORDS
accessory olfactory bulb, chemical communication, immunohistochemistry, lectins, pheromones, vomeronasal organ, vomeronasal system, wolf

1 | INTRODUCTION

After generations of negative interactions between humans and wolves, which have resulted in the decline of wolf populations across most of Europe, new social attitudes towards wildlife and conservation have emerged, leading to the institutionalisation of wolf protection measures (Stohr & Coimbra, 2013). Nevertheless, wolf population control remains a challenging and contentious endeavour. As wolves expand into agricultural regions, human–wolf conflicts intensify. Owing to the wolf's prolific reproductive capacity and tendency to wander, there are few areas where wolves can be reintroduced without some form of population control (Mech, 1995). While lethal measures have historically been employed to mitigate the harm wolves pose to livestock and pets, such measures are becoming less acceptable. However, until non-lethal alternatives become available, lethal methods remain the most effective means to reduce the damages caused by wolves. (Wielgus & Peebles, 2014).

Aversive conditioning (Gustavson & Nicolaus, 1987) has not proven successful with wild wolves (Fritts et al., 1992). Meanwhile, the use of semiochemicals—either pheromones or kairomones (Fortes-Marco et al., 2015)—as a potential population control method has received limited attention (Petrulis, 2013; Riddell et al., 2021; Van Den Berghe et al., 2019). Chemical signals play a significant role in intraspecific communication, mediating the sexual behaviour of the species and the associated physiological processes involved in reproduction. The wolf utilises scent marks to establish territory (Barja et al., 2004; Peters & Mech, 1975), synchronise reproduction (Rothman & Mech, 1979) and convey social status (Barja et al., 2008). Scent marking is primarily observed in mating males and females within a pack, with subordinates only resorting to it during dominance disputes (Asa et al., 1990). This form of social suppression of reproduction is common among wild canids (Macdonald et al., 2019) and extends to rodents like the naked mole-rat, where it is mediated by semiochemicals sensed via a functional vomeronasal organ (VNO) (Dennis et al., 2020).

Despite being a preeminent symbol among endangered species, wolves are among the most extensively studied wild mammals. However, beyond territory-related pheromones in urine and faecal marks (Barja et al., 2004, 2008; Raymer et al., 1985, 1986; Wirobski et al., 2021), there is a surprising lack of research on the neuroanatomical and physiological bases of their chemical communication systems—both the olfactory and vomeronasal systems responsible for processing semiochemicals. To the best of our knowledge, there exists no description of the vomeronasal system (VNS) in the wolf, and information regarding the main olfactory system (MOS) is confined to comparative morphological and neurochemical investigations of the main olfactory bulb (MOB) in domestic and wild canids (Ortiz-Leal, Torres, López-Callejo, et al., 2022).

The MOS comprises millions of neuroreceptor cells situated in the olfactory epithelium covering the olfactory turbinates (Barrios, Sanchez Quinteiro, & Salazar, 2014; Bressel et al., 2016). These cells are responsible for transmitting olfactory information to the MOB

(Doucette et al., 1983; Su et al., 2009). Given its close connection with the limbic system, the MOS has been linked to memory and conscious sensory perception (Slotnick, 2001; Ubeda-Bañon et al., 2011). In contrast, the VNO, a sensorial component of the VNS (Kratzing, 1971; Tomiyasu et al., 2022), contains neuroreceptor cells that transmit signals via the vomeronasal nerves (NVN) (McCotter, 1912; Smith et al., 2015) to the accessory olfactory bulb (AOB) (Frahm & Bhatnagar, 1980; Mohrhardt et al., 2018). The VNS specialises in detecting pheromones (Kunkhyen et al., 2017; Powers & Winans, 1975), kairomones (Fortes-Marco et al., 2013; Isogai et al., 2011) and molecules of the major histocompatibility complex (Leinders-Zufall et al., 2000, 2014). Its functions encompass non-conscious roles in socio-sexual behaviours (Abellán-Álvaro et al., 2022; Baum & Cherry, 2015), maternal recognition (Kohl et al., 2017; Navarro-Moreno et al., 2020), sickness avoidance behaviour (Boillat et al., 2015; Bufe et al., 2019) and predator detection (Tsunoda et al., 2018).

While extrapolations from other species can be problematic when studying the neuroanatomy of the VNS (Salazar & Sánchez-Quinteiro, 2009), the Rodentia Order has served as a major referent for VNO research on mammalian species (Salazar et al., 2013). Consequently, available neuroanatomical data on the VNS of canids is predominantly focused on the domestic dog's VNO (Dennis et al., 2003; Mahdy et al., 2019; Salazar et al., 2013) and AOB (Jawlowski, 1956; Miodonski, 1968; Nakajima et al., 1998; Salazar, Cifuentes, Sánchez Quinteiro, & García Caballero, 1994), along with their secondary projections to the vomeronasal amygdala. Concerning wild canids, until recently, the primary body of research was limited to the study of the rhinencephalon in the African wild dog *Lycaon pictus* brain by Chengetanai et al. (2020) and research on the vomeronasal amygdala in the fox (Równiak et al., 2022; Równiak & Bogus-Nowakowska, 2020). However, a recent comprehensive investigation of the VNO, MOB, AOB and olfactory limbus in the red fox (Ortiz-Leal et al., 2020; Ortiz-Leal, Torres, López-Callejo, et al., 2022; Ortiz-Leal, Torres, Villamayor, et al., 2022) has revealed significant deviations in neuroanatomical structure compared to that observed in the canine VNS. Dogs exhibit noteworthy limitations in the development of the VNO epithelium, inadequate differentiation of the glomerular and nerve layers of the AOB, the smaller size of the VNO and the absence of the characteristic cytoarchitecture found in other mammalian species (Meisami & Bhatnagar, 1998). In contrast, fox studies report a highly differentiated VNS with unique features not documented in the dog, particularly at the VNS level. Likewise, in the case of the African wild dog, the level of development observed in the AOB suggests heightened sensitivity compared to domestic dogs (Chengetanai et al., 2020). All these anatomical differences lend support to the current hypothesis that the domestication of the dog has led to a regression in the detection of pheromones and other semiochemicals, mediated by the VNS.

However, it remains an ongoing question whether, over approximately 10,000 years that separate the wolf and the dog phylogenetically (Bergström et al., 2022; Graphodatsky et al., 2008), the intense selection pressure associated with domestication may have brought

about alterations to the configuration of neural structures that support species-specific behaviours, as is the case with the VNS. As such, this study aims to not only address the significant gap in our morphological and immunohistochemical understanding of the vomeronasal system of the wolf but also shed light on how the domestication process may have impacted the organisation of the central nervous system. We employed various tissue dissection and micro-dissection techniques and computed tomography imaging, followed by general and specific histological staining methods, including immunohistochemical and lectin histochemical labelling techniques.

Among the array of antibodies used for the immunohistochemical analysis of the wolf's VNS, particular attention should be paid to the study of the G protein expression pattern in the sensory epithelium of the VNO, the vomeronasal nerves and the AOB. The immunohistochemical characterisation of both Gαi2 and Gαo G proteins is widely regarded as an excellent phenotypic indicator of the expression of the two main families of vomeronasal receptors, V1R and V2R, respectively, within the VNS. The concurrent expression of both G proteins is a feature observed in Rodentia, including mice, rats, octodons (Suárez & Mpodozis, 2009), guinea pigs (Takigami, 2004) and capybaras (Suárez, Santibáñez, et al., 2011; Torres et al., 2020); Lagomorpha, such as rabbits (Villamayor et al., 2020); Marsupialia, including opossums (Halpern et al., 1995) and wallabies (Torres et al., 2022); and Tenrecidae (Suárez et al., 2009). However, in other mammals, such as the dog, cat, sheep and goat, the differential expression of G proteins and vomeronasal receptors has not been observed, as these species exclusively express the V1R receptor family (Salazar et al., 2007, 2013; Salazar & Sánchez-Quinteiro, 2011; Takigami, 2004). The absence of V2R receptors has been theorised to result from the domestication process, during which artificial selection may have led to an involution of the VNS in canids (Barrios, Sanchez-Quinteiro, & Salazar, 2014; Jezierski et al., 2016). Therefore, investigating the expression patterns of these receptors and the overall anatomy of the VNS in a wild canid with close phylogenetic proximity to the dog, such as the wolf, could provide deeper insights into this theory.

2 | METHODS

In this study, we utilised a sample of five adult male wolves. These wolves originated from wildlife recovery centres in the provinces of Galicia and were unfortunately involved in fatal traumatic accidents. Only those that had died recently and displayed no external or internal head injuries were included in our research. All samples were used with the compulsory permissions by the Galician Environment, Territory and Tenement Council (CMATV approval numbers EB-009/2020 and EB-007/2021).

All the heads were dissected as soon as they arrived at the Faculty of Veterinary, unless one head that was frozen and transverse-sectioned, to compose a macroscopic photographic series. The rest of the heads were dissected extracting the whole brains after opening dorsally the cranium and removing the lateral walls of both the cranial cavity and the ethmoidal fossa with the help of an electric

plaster cutter and a gouge clamp. The VNOs were identified after removing the nasal bones and the lateral walls of the nasal cavity. The bone tissue surrounding the VNO ventrally and medially was dissected from all samples, unless one sample which was decalcified for 2 weeks to microscopically study the topographic relationship of the VNO with the incisive duct. The decalcifying agent used was Shandon TBD-1 Decalcifier (Thermo), and it was applied while stirring continuously at room temperature.

All the samples were fixed in Bouin's fluid (BF) for 24 h, then transferred to 70% ethanol, embedded in paraffin and cut by a microtome. The olfactory bulbs were cut transversely and sagittally by a microtome with a thickness of 8 μm, whereas the VNO samples were sectioned with a thickness of 6–7 μm. The VNO was serially transverse-sectioned along its entire length, from caudal to rostral. The slides were stained using haematoxylin–eosin, Alcian Blue (AB) and Gallego's Trichome stains (Ortiz-Hidalgo, 2011). The staining protocols are explained in detail in Salazar et al. (2003) and Torres, Ortiz-Leal, Ferreiro, et al. (2023).

2.1 | Computed tomography scans

Computed tomography of the head was performed in a 16-slice helical multidetector scanner (Hitachi Eclos 16), obtaining both bone and soft tissue algorithm series in sternal recumbency. For the bone series, a 1.25-mm slice thickness every 0.625 mm, while for the soft tissue series, a 2.5-mm slice thickness every 1.25 mm was applied. Exposure factors were 120 kVp and 200 mA, with 1 s per rotation and a pitch of 0.5.

2.2 | Lectin histochemistry protocol

Lycopersicon esculentum agglutinin (LEA) and the B4 subunit from *Bandeiraea simplicifolia* lectin (BSI-B$_4$) were employed as biotinylated conjugates. Deparaffinised and rehydrated slides were incubated in a solution of 3% hydrogen peroxide to quench endogenous peroxidase activity. Following this, the sections were incubated in a 2% solution of bovine serum albumin (BSA) in 0.1 M phosphate buffer (PB) at pH 7.2 for 30 min. Overnight incubation was performed with LEA and BSI-B$_4$ lectins, separately, in a 0.5% BSA mixture. After two brief washes in PB, the slides were incubated in avidin–biotin–peroxidase (ABC) complex (Vector Laboratories) at room temperature for 90 min. A 0.003% hydrogen peroxide and 0.05% 3,3-diaminobenzidine (DAB) solution in a 0.2 M Tris–HCl buffer were used to visualise the ensuing reaction, which resulted in a brown-coloured deposit.

For *Ulex europaeus* lectin (UEA), the initial two steps mirrored those used for LEA and BSI-B$_4$. Slides were subsequently incubated for 60 min in a 0.5% BSA–UEA mixture. Then, anti-UEA peroxidase-conjugated antibody was added, and overnight incubation ensued. The reaction was revealed through the application of a DAB solution, as described for the LEA and BSI-B$_4$ procedure.

As controls, tests without lectin addition and also pre-absorbed lectins with excessive corresponding sugars, were performed.

2.3 | Immunohistochemistry methodology

The first step involved treating all samples with a 3% hydrogen peroxide solution to inhibit endogenous peroxidase. Subsequently, samples were immersed in either a 2.5% horse serum solution, compatible with the ImmPRESS Anti-Mouse/Anti-Rabbit IgG reagent kit (Vector Laboratories), or 2% BSA for half an hour to preclude non-specific binding. Samples were incubated overnight at 4°C with the primary antibodies (Table 1). The next day, depending on the blocking agent used, samples were incubated for 30 min with either the ImmPRESS VR Polymer HRP Anti-Rabbit IgG or Anti-mouse IgG reagents, with the exception of samples treated with anti-OMP antibodies derived from goats, which were first incubated in a biotinylated anti-goat IgG and afterwards incubated in ABC reagent for 1.5 h under humid conditions. Three sequential 5-min PB washes were carried out between steps. Prior to the visualisation stage, all samples were rinsed for 10 min in 0.2 M Tris–HCl buffer at pH 7.61. DAB chromogen was used for visualising, following the same protocol used for lectin histochemical labelling. Negative controls omitted the primary antibodies.

2.4 | Double immunohistochemical protocol for paraffin-embedded tissue

For double immunostaining, a sequential twice-repeated enzyme-labelled method was employed (Hasui et al., 2003; Villamayor et al., 2020). Between both immunolabelling, the sections were subjected to treatment with 0.1 M glycine solution (pH 2.2) for 5 min. To select the most suitable dye to visualise the immunoreaction, both DAB and Vector VIP Peroxidase Substrate Kit (SK-4600, Vector Laboratories) were combined exchanging their order.

2.5 | Image capture

Images were digitally captured using a Karl Zeiss Axiocam MRc5 camera coupled with a Zeiss Axiophot microscope. Adobe Photoshop CS4 was employed for brightness, contrast and balance adjustment; however, no enhancements, additions or relocations of the image features were made. Additionally, an image-stitching software (PTGuiPro) was used for low magnification images composed of several photographs.

3 | RESULTS

The VNS was studied at both the macroscopic and microscopic levels. For each of these levels, detailed descriptions of the vomeronasal organ, vomeronasal nerves and AOB are provided.

3.1 | Macroscopic study of the VNS

3.1.1 | Vomeronasal organ (Figures 1–5)

As a preliminary step towards dissecting the vomeronasal organ, a cross sectional macroscopic anatomical study of the nasal cavity was performed on a single specimen (Figure 1a–e). Eight sections were selected, spanning from the nasal vestibule to the ethmoid turbinates (Figure 1c), with the section corresponding to level 6 encompassing the central part of the VNO (Figure 1b,d). At higher magnification, the VNO corresponds to two tubular structures located in the ventral region of the nasal septum, laterally to the vomer bone and ventrally to the cartilage of the nasal septum (Figure 1b). Enveloping the VNO is a cartilaginous capsule (indicated by arrowheads), which fully surrounds the parenchyma of the organ, except for its dorsal region. In its central part, the vomeronasal ducts are clearly visible (Figure 1d).

The study of the topographic relationships of the vomeronasal organ was expanded to computed tomography scans, which provided clear images of the head cavities including the nasal turbinates, nasal meatuses, teeth, vomer bone and nasal septum. Special attention was given to the bony configuration of the vomer bone and palatine fissure (Figure 2a), as previous anatomical studies of the nasal cavity have shown that the VNO is located on the lateral surface of the vomer. The results of the study are presented in three computed tomography sections: horizontal (Figure 2b), sagittal (Figure 2c) and transverse (Figure 2d). In all three planes, levels, including the VNO, have been chosen. The vomeronasal organ is situated bilaterally on each side of the vomer bone, positioned at the most rostral and ventral regions of the nasal cavity. It occupies a narrow compartment located dorsomedially to the palatine fissure, extending to the level of the root of the upper canine tooth.

To access the VNO, it was necessary to expose the nasal septum. First, the lateral wall of the cavity formed by the maxillary bone was removed. Then, the large ventral nasal turbinate was extracted (Figure 3). In the basal region of the septum, the VNO lies, covered by the respiratory mucosa layer. The caudal nasal myelinated nerve, which enters the VNO at its most caudal extremity (Figure 3a), serves as a reliable indicator of the VNO's location. On the mucosal surface of the nasal septum, amyelinic fibres of the vomeronasal nerve can be seen running in a caudodorsal direction towards the lamina cribrosa of the ethmoid. In their most rostral segment, the NVN are in direct contact with the respiratory mucosa, and more caudally, they extend into the olfactory mucosa, which is easily distinguished by its yellowish colour (Figure 3b). By removing the lateral wall of the cranial cavity, the size of the telencephalon and the location of the olfactory bulb can be determined (Figure 3c).

Before the removal of the VNO, the nasal cavity was reduced to small blocks, which contain the ventral part of the nasal septum and the bony floor of the palate. This allowed for a clearer verification of the relationship between the VNO and the nasal

TABLE 1 Specifications for each antibody used in this study, encompassing supplier information, dilution ratios, target immunogens and Research Resource Identifiers (RRID).

Antibody	First Ab species/ dilution	First Ab catalogue number/Manufacturer	Immunogen	Reference	RRID	Second Ab species/dilution, catalogue number
Anti-Gαo	Rabbit 1:200	MBL-551	Bovine GTP binding protein Gαo subunit	Prince et al. (2009)	AB_591430	ImmPRESS VR HRP Anti-rabbit IgG Reagent MP-6401-15
Anti-Gαi2	Rabbit 1:200	Santa Cruz Biotechnology sc-7276	Peptide mapping within a highly divergent domain of Gαi2 of rat origin	de la Rosa-Prieto et al. (2010)	AB_2111472	ImmPRESS VR HRP Anti-rabbit IgG Reagent MP-6401-15
Anti-CB	Rabbit 1:6000	Swant CB38	Rat recombinant calbindin D-28k	Alonso et al. (2001)	AB_10000340	ImmPRESS VR HRP Anti-rabbit IgG Reagent MP-6401-15
Anti-CR	Rabbit 1:6000	Swant 7697	Recombinant human calretinin containing a 6-his tag at the N-terminus	Crespo et al. (1997)	AB_2619710	ImmPRESS VR HRP Anti-rabbit IgG Reagent MP-6401-15
Anti-OMP	Goat 1:400	Wako 544–10001	Rodent olfactory marker protein	Verhaagen et al. (1990)	AB_839504	ImmPRESS VR HRP Anti-mouse IgG Reagent MP-6402–15
Anti-GAP43	Mouse 1:400–1:4000	Sigma G9264	HPLC-purified GAP43 from neonatal rat forebrain	Villamayor et al. (2021)	AB_477034	ImmPRESS VR HRP Anti-mouse IgG Reagent MP-6402–15
Anti-MAP2	Mouse 1:200	Sigma M4403	Rat brain microtubule-associated proteins	Tran et al. (2008)	AB_477193	ImmPRESS VR HRP Anti-mouse IgG Reagent MP-6402–15
Anti-GFAP	Rabbit 1:200	DAKO Z0334	GFAP isolated from cow spinal cord	Bignami et al. (1972)	AB_10013382	ImmPRESS VR HRP Anti-rabbit IgG Reagent MP-6401-15

Note: In all cases, the immunoreactivity patterns observed in wolf samples were consistent with those previously documented across various mammalian species. Relevant references for each antibody are included.

Abbreviations: ABC, avidin–biotin-complex; CB, calbindin; CR, calretinin; GAP-43, growth-associated protein 43; GFAP, glial fibrillary protein; Gαi2, Subunit αi2 of G protein; Gαo, Subunit αo of G protein; HRP, horseradish peroxidase; IgG, immunoglobulin G; MAP-2, microtubule associated protein; OMP, olfactory marker protein.
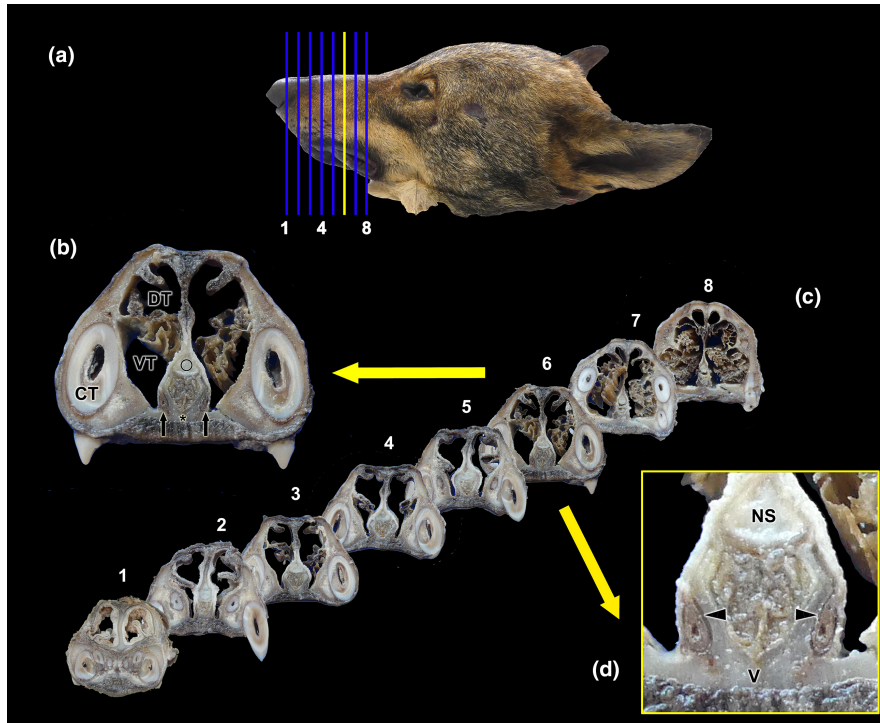
FIGURE 1 Macroscopic cross sectional study of the nasal cavity of the wolf. (a) Lateral view of the head of the wolf showing the eight consecutive levels chosen for the macroscopic sectional study. (b) The central part of the vomeronasal organ (VNO) is located at level 6 (yellow line in "a", enlarged section in "b and d"). The VNO corresponds to two tubular structures located in the ventral part of the nasal septum (black arrows), lateral to the vomer bone (asterisk) and ventral to the cartilage of the nasal septum (circle). (c) Transverse sections of the nasal cavity ordered from rostral (1) to caudal (8), corresponding to the levels represented in (a). (d) At higher magnification, it can be seen how the VNO is enveloped by a cartilaginous capsule (arrowheads). In the central part of the VNO, the vomeronasal ducts can be observed. CT, canine tooth; DT, dorsal turbinate; NS, nasal septum; VT, ventral turbinate.
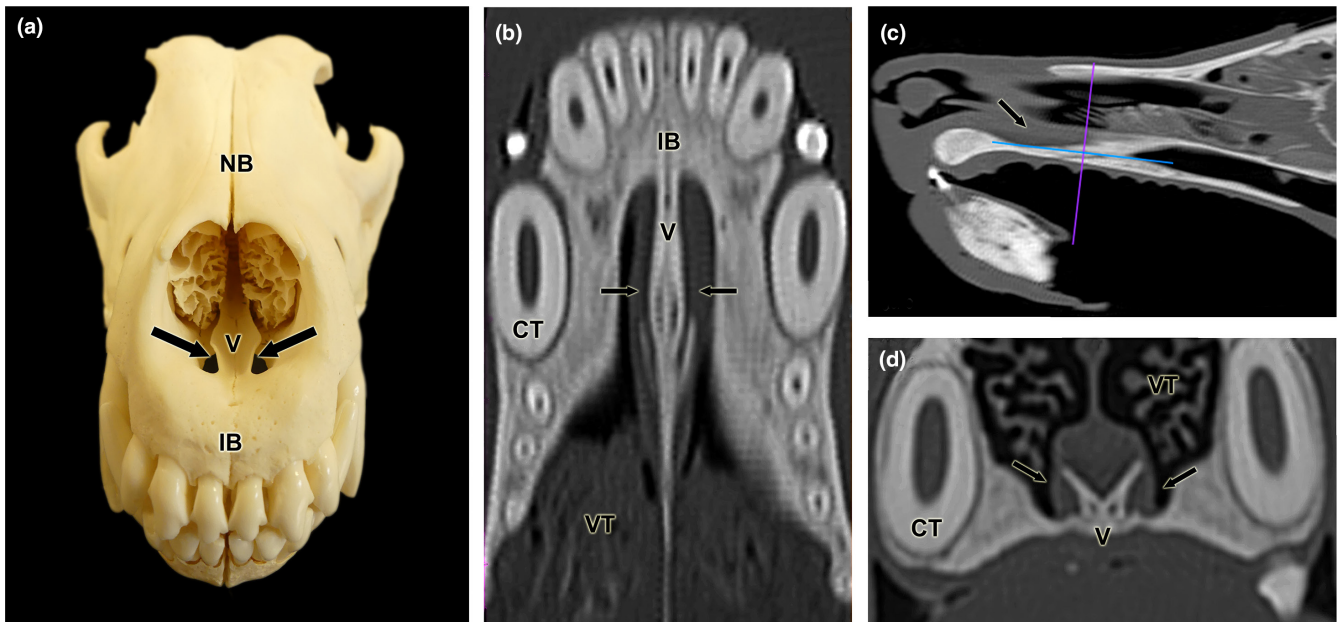
FIGURE 2 Topographical relationship of the wolf VNO. (a) Fronto-dorsal view of the skull skeleton showing the relationship of the lateral part of the vomer bone (V) to the palatine fissure. (b–d) Computerised tomography images of the head in the horizontal (b), parasagittal (c) and transverse (d) planes. Arrows indicate the location of the VNO. CT, canine tooth; IB, incisive bone; NB, nasal bone; VC, vomeronasal cartilage; VT, ventral turbinate.
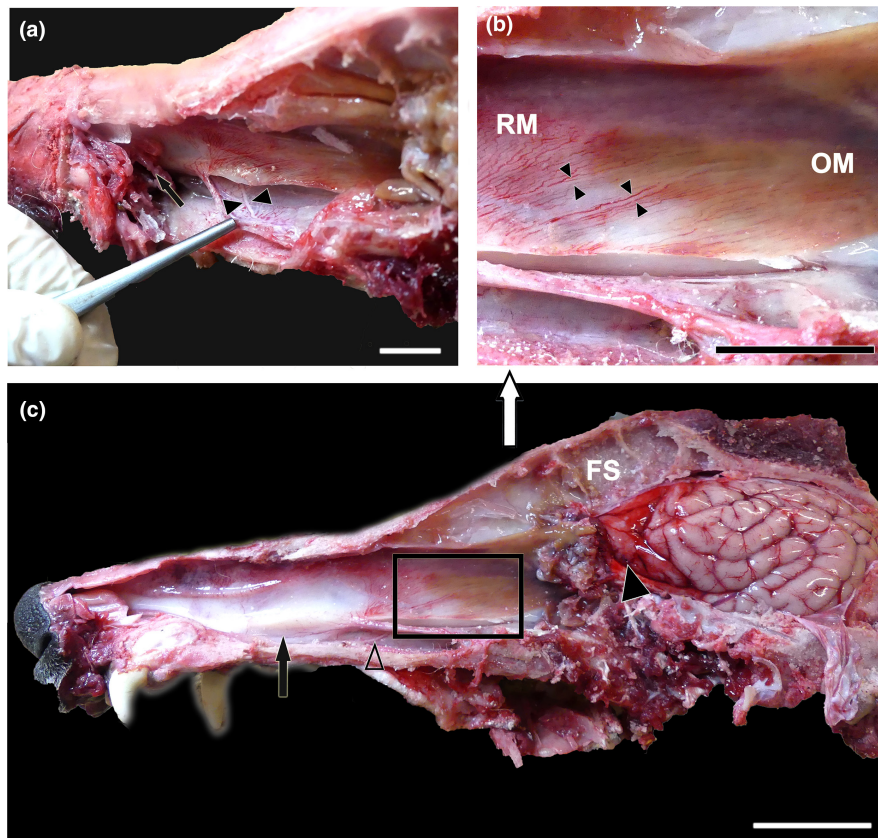
FIGURE 3 Dissection of the nasal and cranial cavities of the wolf. (a). Dorsolateral view of the nasal cavity, showing the projection zone of the VNO (arrow) and the myelinated branches forming the caudal nasal nerve (arrowheads) entering the VNO. (b) Enlargement of the inset shown in (c) displaying the vomeronasal nerves leaving the VNO (arrowheads) in a caudodorsal direction towards the medial portion of the cribriform plate of the ethmoid. RM: Respiratory mucosa. OM: Olfactory mucosa. (c) Lateral view of the nasal and cranial cavities, showing in the latter the left-brain hemisphere. The projection area of the VNO (arrow), the vomeronasal nerves in a caudodorsal direction (inset), the caudal nasal nerve (open arrowhead) and the olfactory bulb (arrowhead) are also indicated. FS, Frontal sinus. Scale bar=1.5 cm.
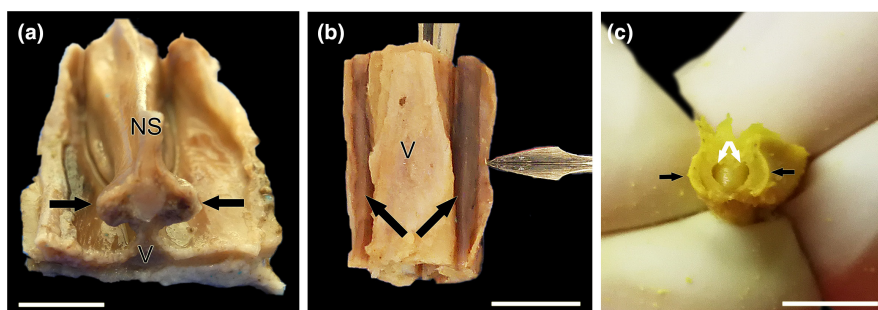

FIGURE 4 Wolf VNO after its full extraction in association to the vomer bone. (a) Transverse cross section of the nasal septum corresponding to the level 9 shown in Figure 1. From a caudodorsal viewpoint, the VNOs (arrows) are visualised on both sides of the base of the nasal septum (NS) over the thin vertical projection of the vomer bone (V). (b) On a more rostral level, corresponding to level 3 of Figure 1, a ventral view of the vomer bone shows both VNOs with its distinctive rounded and elongated shape (arrows). The lancet points to the lifted respiratory mucosa of the nasal cavity that covers the VNO. (c) Dissected out and partially transversely sectioned VNO (black arrows) showing the crescent shape vomeronasal duct (white arrows). a and b, fresh samples; (c), BF-fixed sample. Scale bars: (a–b)=0.5 cm, (c)=0.2 cm.

septum. At a caudal level, the VNO is located on both sides of the base of the nasal septum. It is positioned relatively high, given the vomer bone's vertical projection (Figure 4a). At more rostral levels, the VNO is perfectly adapted to the lateral curvature of the vomer bone, allowing for easy access from a ventral direction. By excising the respiratory mucosa laterally overlying the VNO

within the nasal cavity, its shape and development can be visualised (Figure 4b). Finally, the VNO was dissected from the surrounding bone tissue, where it is held by dense connective tissue. To confirm the VNO's identity, a transverse cut was made in the sample, revealing the vomeronasal duct and the organ's parenchyma (Figure 4c).
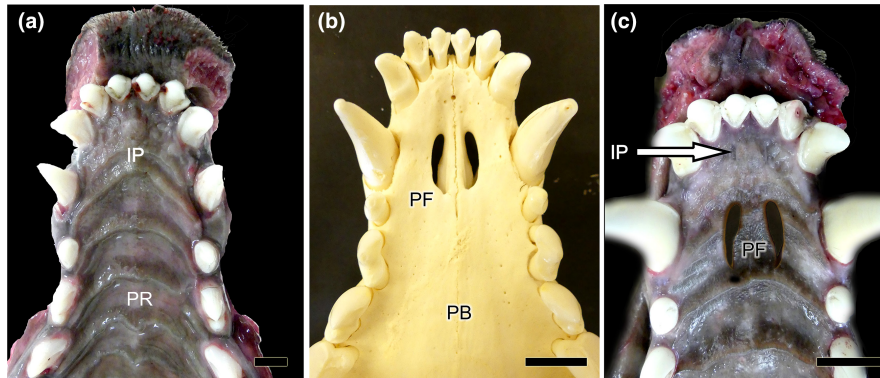
FIGURE 5 Ventral view of the palate of the wolf after removal of the mandible. (a) The mucosa of the roof of the oral cavity is observed, and in its most anterior part, the location of the incisive papilla (IP) and palatine rugae (PR) are indicated. (b) Skeleton of the corresponding area where the palatine fissures (PF) are observed on both sides of the midline. PB: Palatine bone. (c) Superposition of images analogous to "a and b" to show the exact location of the PF on the mucosa of the palate. The IP is also shown (arrow). Scale bar: (a) 1 cm, (b–c) 1.5 cm.
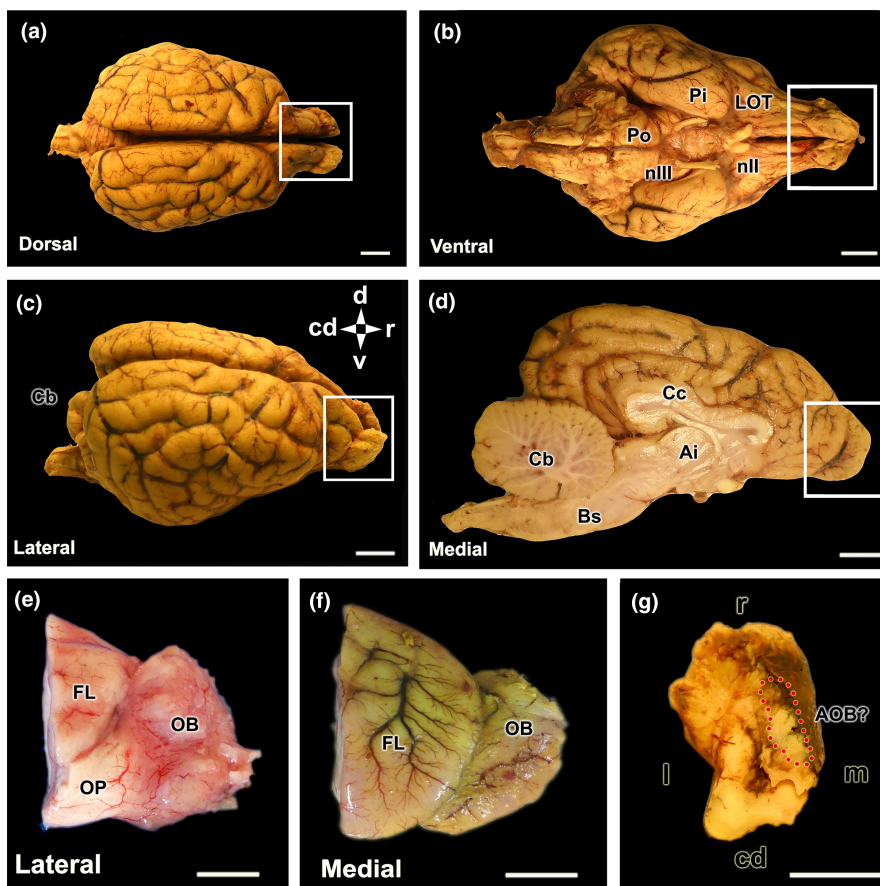
FIGURE 6 Encephalon and olfactory bulb of the wolf. (a–d) Dorsal, ventral, lateral and medial views of BF-fixed encephalon. The white box highlights the dorsal, ventral, lateral and medial views of the olfactory bulb (OB) respectively. (e) Lateral view of the right olfactory bulb, separated from a formalin-fixed brain. (f) Medial view of the left MOB separated from the BF-fixed brain. (g) Dorsocaudal view of the left OB, BF fixed. The area where the accessory olfactory bulb is presumptively located is indicated by the broken red circle. Bs, brain stem; Cb, cerebellum; Cc, corpus callosum; Cd, caudal; d, dorsal; FL, frontal lobe; Ia, interthalamic adhesion; l, lateral; LOT, lateral olfactory tract; m, medial; nII, optical nerve; nIII, oculomotor nerve; OP, olfactory peduncle; Pi, piriform lobe; Po, Pons; R, rostral. Scale bar = 1 cm.

To complete the anatomical study of the VNO, we examined its means of communication with the external environment. This communication is essential for the chemical messenger molecules to reach the neurosensory epithelium (Figure 5). The wolf establishes this link indirectly via the incisive duct (ID), which acts as a conduit linking the nasal and oral cavities (Figure 5b). The vomeronasal duct is situated between the two. The incisive papilla connects the ID to the oral cavity (Figure 5c). Microscopic evaluation will be performed to ascertain whether the vomeronasal duct enters the ID, as this cannot be observed macroscopically.
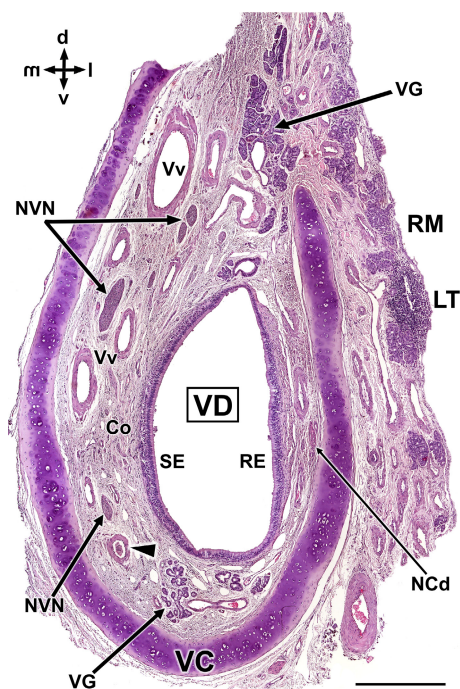
3.1.2 | AOB (Figure 6)

The macroscopic investigation of the wolf's brain reveals well-developed olfactory bulbs that are conspicuous from both the lateral and medial views of the hemiencephalon (Figure 6a–d). Particularly remarkable is the well-developed rhinencephalon, characterised by large olfactory pedunculi (Figure 6e) and broad, convex piriform lobes (Figure 6b).

The main objective of the macroscopic study was to identify the AOB in situ. However, in none of the studied specimens were we able to achieve this identification owing to its reduced dimension and the usual presence of blood clots in the ethmoid fossa. The anatomical tracing of the vomeronasal nerves consistently pointed to an area located in the caudomedial part of the MOB, which was the focus of special attention in the sagittal histologic series of the bulb (Figure 6g).

3.2 | Microscopic study of the VNO (Figures 7–14)

As a preliminary microscopic approximation, the VNO comprises a vomeronasal capsule and a vomeronasal duct, surrounded by parenchyma that contains blood vessels, nerves and vomeronasal
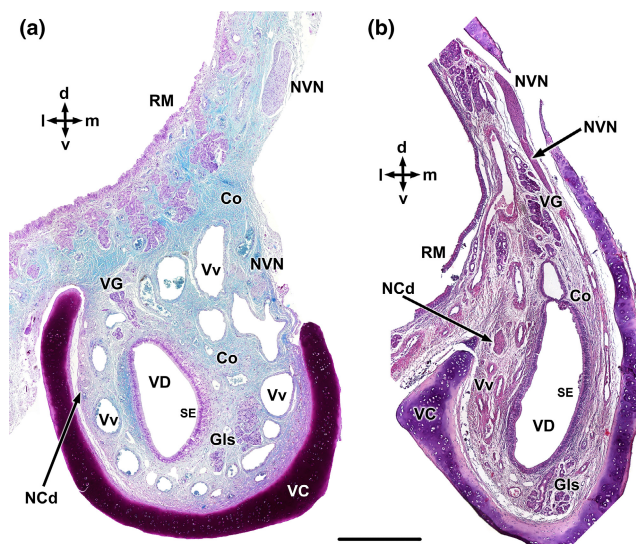
glands (Figure 7). The capsule, comprising hyaline cartilage and adopting a 'U' shape, encases the parenchyma and prevents the lumen from collapsing. The lumen is typically elliptical and lined by pseudostratified epithelium. The epithelium's lateral portion exhibits a respiratory nature, while the medial portion is neuro-sensory in type, with both portions appearing to be of comparable size and development.

The parenchyma of the organ primarily comprises blood vessels, which are evenly distributed around its circumference. However, they are particularly prominent in the dorsal and lateral regions, where numerous large and muscular veins are present. Arteries, meanwhile, are scarce and relatively small. The medial veins are interspersed with numerous branches of the vomeronasal nerves. In the lateral parenchyma, the nerves are of smaller calibre and correspond to branches of the caudal nasal nerve. The glandular component is not very abundant, with the glands concentrated near the ventral and especially dorsal commissures. The dorsal glands extend into the parenchyma of the respiratory mucosa, which itself features profuse irrigation, abundant glandular tissue and diffuse lymphoid tissue. The parenchyma of the VNO is rich in connective tissue.

The histological study encompassed sections from both the rostral and caudal thirds of the VNO (Figure 8). In both segments, the overall organisational pattern of the organ remains consistent. Within the anterior third (Figure 8a), the cartilage is more open dorsally, the venous vessels possess larger calibres but thinner walls, and the nerve branches are less abundant. The distinction between the two epithelia becomes evident. Gallego's trichrome staining reveals the remarkable development of connective tissue. In a more

FIGURE 7 Histological transverse section of the wolf vomeronasal organ in its central portion, stained with haematoxylin–eosin. This central level exemplifies the major histological features of the VNO. VC, vomeronasal cartilage. In its central portion, it forms an incomplete ring which opens dorsally. Arrowhead, artery; Co, connective tissue; D, dorsal; l, lateral; LT, Lymphoid tissue; m, medial; NCd, caudal nasal nerve; NVN, vomeronasal nerves; RE, respiratory epithelium; RM, respiratory mucosa; SE, neurosensory epithelium; v, ventral; VD, vomeronasal duct; VG, vomeronasal glands; Vv, vomeronasal veins. Scale bar = 500 μm.

FIGURE 8 Transverse sections of the wolf VNO at two selected levels. (a) Rostral level. (b) Caudal level. Co, connective tissue; Gls. vomeronasal glands; NCd, caudal nasal nerve; NVN, vomeronasal nerve; RM, respiratory mucosa; SE, Sensory epithelium; VG, vomeronasal glands; VC, vomeronasal cartilage; VD, vomeronasal duct; and Vv, vomeronasal veins. Staining: Gallego's trichrome (a) and haematoxylin–eosin (b). d, dorsal; l, lateral; m, medial; and v, ventral. Scale bar = 500 μm.
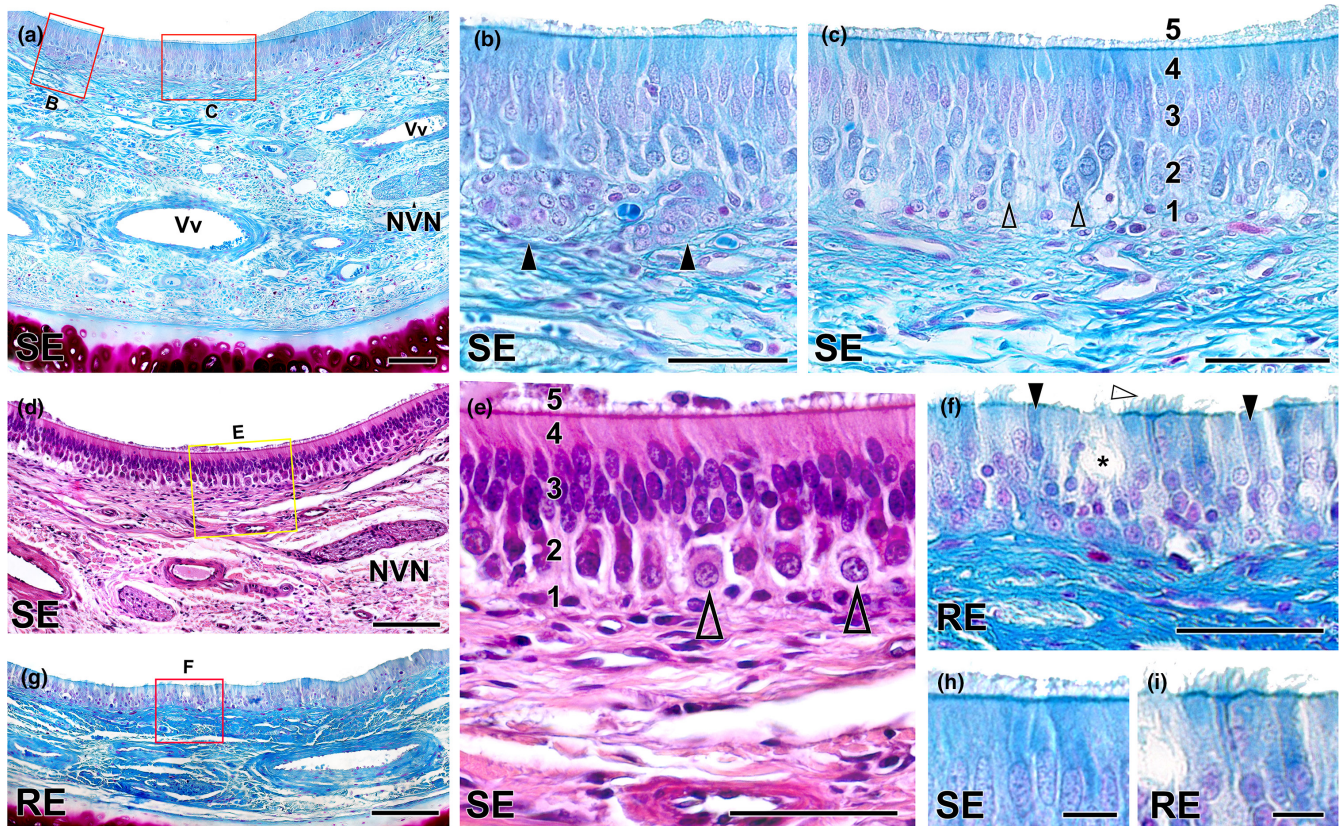
FIGURE 9 Histological study of the epithelia of the wolf vomeronasal duct. (a) Medial parenchyma of the organ stained with Gallego's trichrome. The overlying sensory neuroepithelium (SE), enlarged in (b, c), shows a large lamina propria with veins (Vv), vomeronasal nerves (NVN) and connective tissue. (b) Two large clusters of cells similar in appearance to neuroreceptor cells (arrowheads) are observed in the lamina propria. (c) Cellular components of the neuroepithelium: 1, basal cells; 2, neuroreceptor cells (open arrowheads); 3, sustentacular cells; 4, cell processes layer; and 5, mucomicrovillar complex. (d) Neurosensory epithelium and lamina propria, stained with haematoxylin–eosin. (e) Enlargement of the area is shown in "d" showing the five components of the sensory neuroepithelium. Open arrowheads: neurosensory cells. (f) Enlargement of the area of respiratory epithelium (RE) is shown in (g), stained with Gallego's trichrome. Note the presence of cilia (white arrowhead), chemosensory cells (black arrowheads) and goblet cells (*). (g) Respiratory epithelium stained with Gallego's trichrome. (h) Enlargement of the Figure "c", displaying the luminal surface of the SE, covered by the microvillar complex. (i) Enlargement of the luminal surface of the RE, showing the ciliated covering. Scale bars: (a, d, g) = 100 μm; (b, c, e, f) = 50 μm; (h, i) = 10 μm.
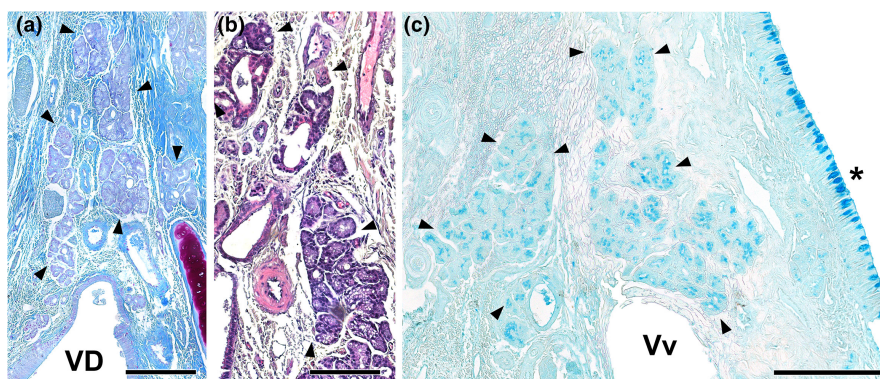
FIGURE 10 Vomeronasal glands of the wolf. The VNO parenchyma presents an abundant number of glands, which are more developed in its dorsal area. (a, b) The arrowheads delimit the glandular areas of interest. Both Gallego's trichrome (a) and haematoxylin–eosin (b) stainings show the serous tubuloalveolar nature of the wolf vomeronasal glands. (c) Alcian blue staining shows the positivity of these acini to this stain. VD, vomeronasal duct; Vv, vomeronasal veins; (*) Respiratory mucosa. Scale bar = 250 μm.

caudal section (Figure 8b), the medial branch of the cartilage shows increased development, assuming a 'J' shape. At this level, the vomeronasal nerves exit the parenchyma from their dorsal extremity, forming large nerve trunks.

The histological examination of the two epithelia lining the vomeronasal duct (Figure 9) was performed using Gallego's trichrome (Figure 9a–c,f–I) and haematoxylin–eosin stains (Figure 9d,e). The broad lamina propria associated with the neuroreceptor
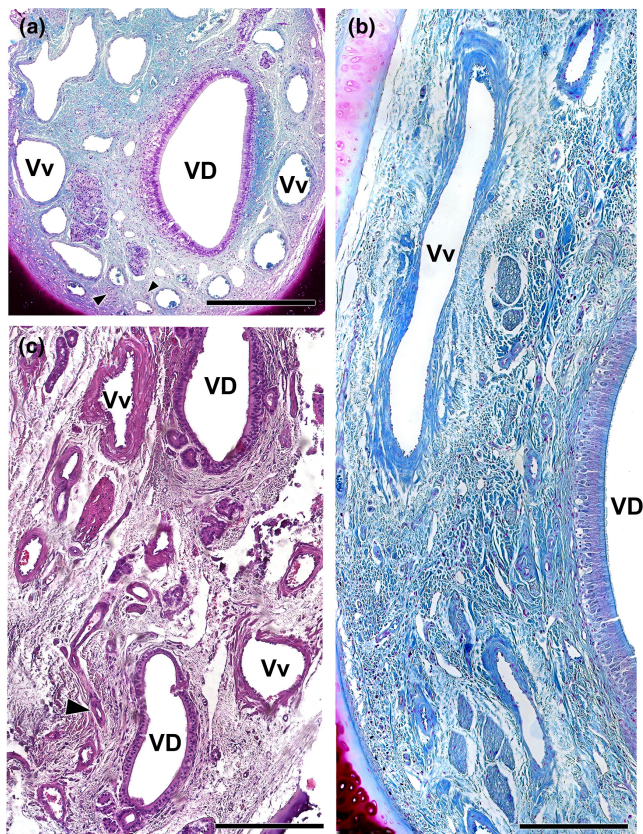
FIGURE 11 Vasculature of the wolf VNO. (a) Image of the anterior portion of the VNO is shown in Figure 8a exemplifies the presence of a profuse venous ring (Vv) surrounding the vomeronasal duct (VD). The arteries (arrowheads) are small and sparse. (b) Arteries indicated in A showed at higher magnification. (c) Caudal section of the VNO showing the glove-fingered termination of the vomeronasal duct (VD). Numerous veins (Vv) and small arterial trunks (arrowhead) predominate at this level. (d) In a central section of the VNO, large venous sinuses (Vv) run along the lateral portion of the parenchyma. NCd, caudal nasal nerve. Staining: (a, b d) Gallego's trichrome; (c) haematoxylin–eosin. Scale bars: (a, d)=250μm; (c)=100μm; (b)=50μm.

epithelium contains abundant connective tissue, with blood vessels and branches of the vomeronasal nerves interwoven within its fibres (Figure 9a). The most striking feature is the presence—in a subepithelial position within the lamina propria—of conspicuous clusters of densely packed cells that traverse the basal cell layer, maintaining a direct relationship with the neuroreceptor cells (Figure 9b). While these cluster-forming cells lack visible processes, their nuclei resemble in shape, content and staining to those of the neuroreceptor cells. To the best of our knowledge, this species stands as the sole example presenting such cellular organisation in the vomeronasal epithelium. Positioned more superficially are the cellular components of the vomeronasal neuroepithelium (Figure 9c,h).

They are organised in a columnar, pseudostratified and non-ciliated epithelium. From basal to luminal, its components are basal cells, neuroreceptor cells, sustentacular cells, the cell processes layer and the superficial mucomicrovillar complex. The neuroreceptor
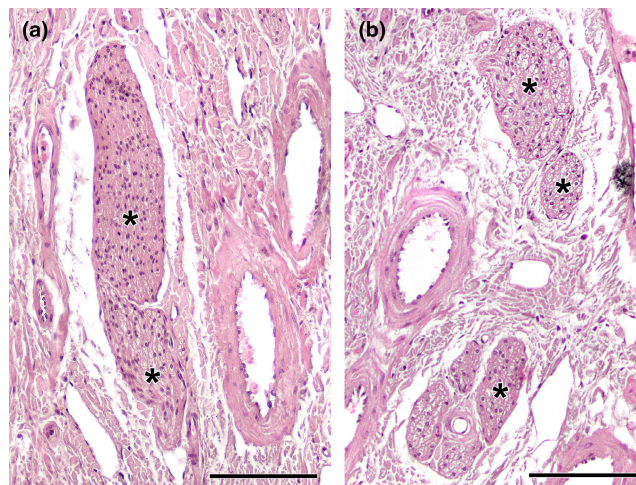

FIGURE 12 Histological study of the wolf vomeronasal organ innervation. (a). Unmyelinated branches of the vomeronasal nerves (*). They are characterised by their homogeneous appearance, with densely packed nerve bundles. (b). The lateral part of the parenchyma contains myelinated nerve branches originating from the caudal nasal nerve (*). Their structure is looser and the void spaces corresponding to the myelin sheaths are visible. Staining: Haematoxylin–eosin. Scale bar=100μm.

cells are ellipsoidal and not densely packed, allowing for the visualisation of their fine axonal and dendritic processes. Their nuclei are rounded and contain visible nucleoli. The sustentacular cells have densely packed nuclei in the apical position and are elongated. Haematoxylin–eosin staining confirmed these observations (Figure 9d,e). The respiratory epithelium (Figure 9f,g,i) is a pseudostratified columnar epithelium that presents cilia on its surface. It consists of sustentacular, chemosensory and goblet cells (Figure 9f).

The VNO parenchyma of the wolf contains numerous glands, with more pronounced development in its dorsal region (Figure 10). Both Gallego's trichrome (Figure 10a) and haematoxylin–eosin (Figure 10b) staining reveal the serous tubuloalveolar nature of the vomeronasal glands. Alcian blue staining demonstrates that the acini secrete an Alcian Blue-positive material (Figure 10c).

The information concerning blood vessels is summarised in Figure 11. These vessels form a large vascular network, providing the organ with erectile tissue functionality. In the anterior portion of the VNO, veins form a complete vascular ring encircling the vomeronasal duct (Figure 11a). In the central area of the VNO, large venous sinuses run along the lateral portion of the parenchyma (Figure 11d). Conversely, in the caudal area of the VNO, where the glove-fingered termination of the vomeronasal duct appears, numerous medium-sized veins predominate (Figure 11c). In contrast, arteries within the VNO are small and sparse (Figure 11b,c).
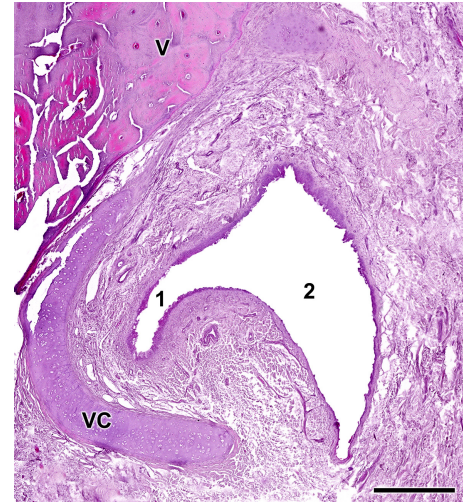
The innervation of the VNO consists of two types of nerves classified according to their myelination (Figure 12). The sensory component comprises unmyelinated branches of the vomeronasal nerves (Figures 7 and 8). These nerves occupy the medial parenchyma of the VNO, characterised by their homogeneous appearance and densely packed nerve bundles (Figure 12a). Meanwhile,
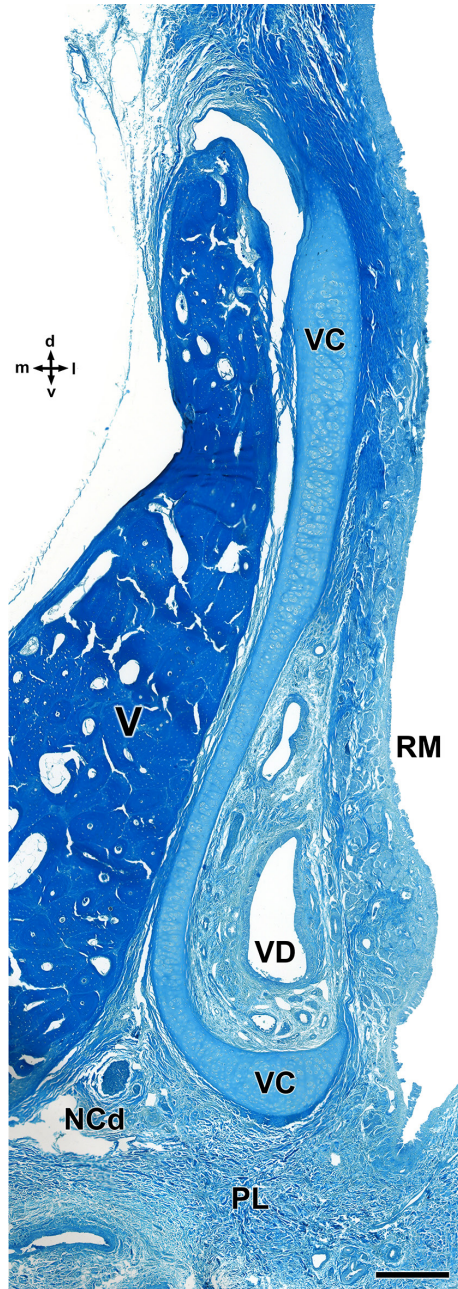
FIGURE 13 Decalcified cross section of the anterior portion of the wolf nasal septum, stained with Gallego's trichrome, showing the topographical relationship of the VNO with the vomer bone. The vomeronasal cartilage (VC) presents an elongated morphology, accompanying the shape of the vomer bone (V) and opens laterally. d, dorsal; l, lateral; LP, lamina propria; m, medial; NCd, caudal nasal nerve; PL, palate; RM, respiratory mucosa; v, ventral; VD, vomeronasal duct. Scale bar = 250 μm.
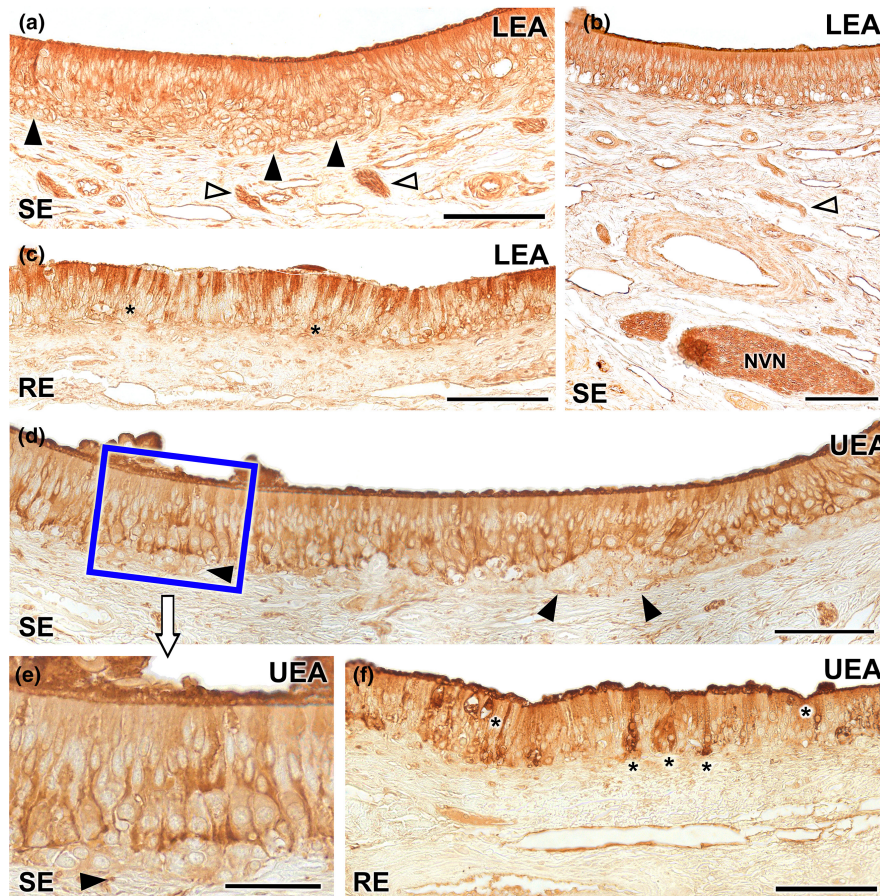

FIGURE 14 Opening of the vomeronasal duct into the incisive duct of the wolf. The vomeronasal duct (1) establishes a direct communication with the incisive duct (2). Anatomically, the latter runs laterally to the organ, allowing a double direct communication between the oral and nasal cavities. Staining: haematoxylin–eosin. VC, vomeronasal cartilage; and V, vomer bone. Scale bar = 500 μm.

rostral part of the nasal septum. These sections illustrate the topographical relationship of the rostral VNO with the vomer bone (Figure 13). At this level, the vomeronasal cartilage assumes an elongated morphology that aligns with the shape of the vomer bone, featuring a notable lateral gap. Further examination of more rostral decalcified samples confirmed, microscopically, the functional communication of the vomeronasal duct with the external environment via the ID. The latter runs laterally to the VNO, facilitating direct communication between the vomeronasal duct and both the oral and nasal cavities. It achieves this by opening ventrally into the aperture present in the elevated mucosa, forming the incisive papilla, and dorsally into the meatus located on the floor of the nasal cavity (Figure 14).

3.3 | Lectin histochemical study of the VNO (Figure 15)

Both the neuroreceptor cells of the sensory epithelium and the vomeronasal nerves of the VNO show positive histochemical labelling for both UEA and LEA lectins (Figure 15). However, when considering the neuroepithelial cell clusters located in the basal region of the neuroepithelium, both lectins exhibit contrasting labelling patterns.

While LEA produces positive labelling of neuronal clusters (Figure 15a), UEA lectin does not label these cells (Figure 15d,e). LEA labelling is slightly more pronounced in the apical processes of the epithelium (Figure 15a,b), while UEA produces more intense labelling in the basal regions of the epithelium (Figure 15d,e), excluding the unlabelled clusters. Regarding the respiratory epithelium, it exhibits diffuse labelling from both lectins, albeit with distinct patterns. LEA positivity is primarily concentrated in most of the apical processes of

the lateral portion of the parenchyma contains myelinated nerve branches originating from the caudal nasal nerve (Figures 7, 8b and 11d). These branches exhibit a more loosely structured appearance, and the empty spaces corresponding to the myelin sheaths can be seen (Figure 12b).

Our microscopic investigation of the VNO was complemented by an examination of decalcified histological sections from the

FIGURE 15 Lectin histochemical labelling of the vomeronasal epithelium. (a–c) LEA lectin labelling: The neuroreceptor epithelium (SE) shows intense labelling throughout all its components including neuroepithelial clusters (black arrowheads) and nerve bundles in the lamina propria (white arrowheads) (a). This labelling extends to the vomeronasal nerves (NVN) (b). (c) The respiratory epithelium shows a diffuse LEA positivity, concentrated mainly in the most apical part of the epithelium, while the basal cells remain unlabelled (asterisk). (d–f) UEA lectin: Positivity is demonstrated across the sensory epithelium of the VNO excluding the neuronal clusters (arrowheads) which are not labelled (d). At higher magnification, an intensity gradient increasing with depth can be discerned (e). The unlabelled neuronal clusters are shown (arrowhead). (f) The respiratory epithelium exhibits fainter labelling, with few positive cells scattered along the epithelium (*). UEA labelling is also markedly concentrated in the mucociliary layer. Scale bar: (a–d, f)=100 μm; (e)=50 μm.

the epithelium (Figure 15c), while UEA presents a few strongly labelled cells scattered along the epithelium. Within the mucociliary complex, labelling is stronger with UEA compared to LEA (Figure 15f).

3.4 | Immunohistochemical study of the VNO (Figures 16 and 17)

The anti-Gαo antibody, which specifically labels the αo subunit of the G protein transduction cascade associated with the V2R receptor, labels a subpopulation of neurons predominantly located in the basal layers of the neuroepithelium. This arrangement is more evident in those areas of the epithelium with a greater number of layers of neuroreceptor cells. These neurons extend their axons towards the adjacent vomeronasal nerves (Figure 16a,b). The labelling encompasses the entire length of the immunopositive neuroreceptor cells, spanning from the apical dendrite to the soma. Furthermore, immunopositive neuroreceptor cells embrace the intra-epithelial capillaries of the

VNO (Figure 16c). The anti-Gαi2 antibody, which labels the αi2 subunit of the G protein transduction cascade linked to the V1R receptors, labels neuroreceptor cells predominantly present in the central region of the epithelium and within the vomeronasal nerves (Figure 16d,e). In contrast to Gαo, no immunopositive neurons are identified in proximity to the intra-epithelial capillaries. Neither anti-Gαo nor anti-Gαi2 immunolabel the entirety of the dendritic processes that constitute the apical surface of the epithelium, suggesting the complementarity of both immunolabelling. Additionally, the dendritic knobs, immunolabelled with anti-Gαi2, while less numerous than those labelled by anti-Gαo, exhibit a more dilated morphology (Figure 16e). The deep neuronal clusters remain immunonegative.

To accurately verify the complementarity of both neuroreceptor cell subpopulations based on their immunostaining against G proteins subunits, we performed a double immunohistochemical labelling against both G proteins. This technique revealed the presence of both cellular subpopulations, differentiated by the immunostaining at the level of both neuronal somas and dendritic buttons
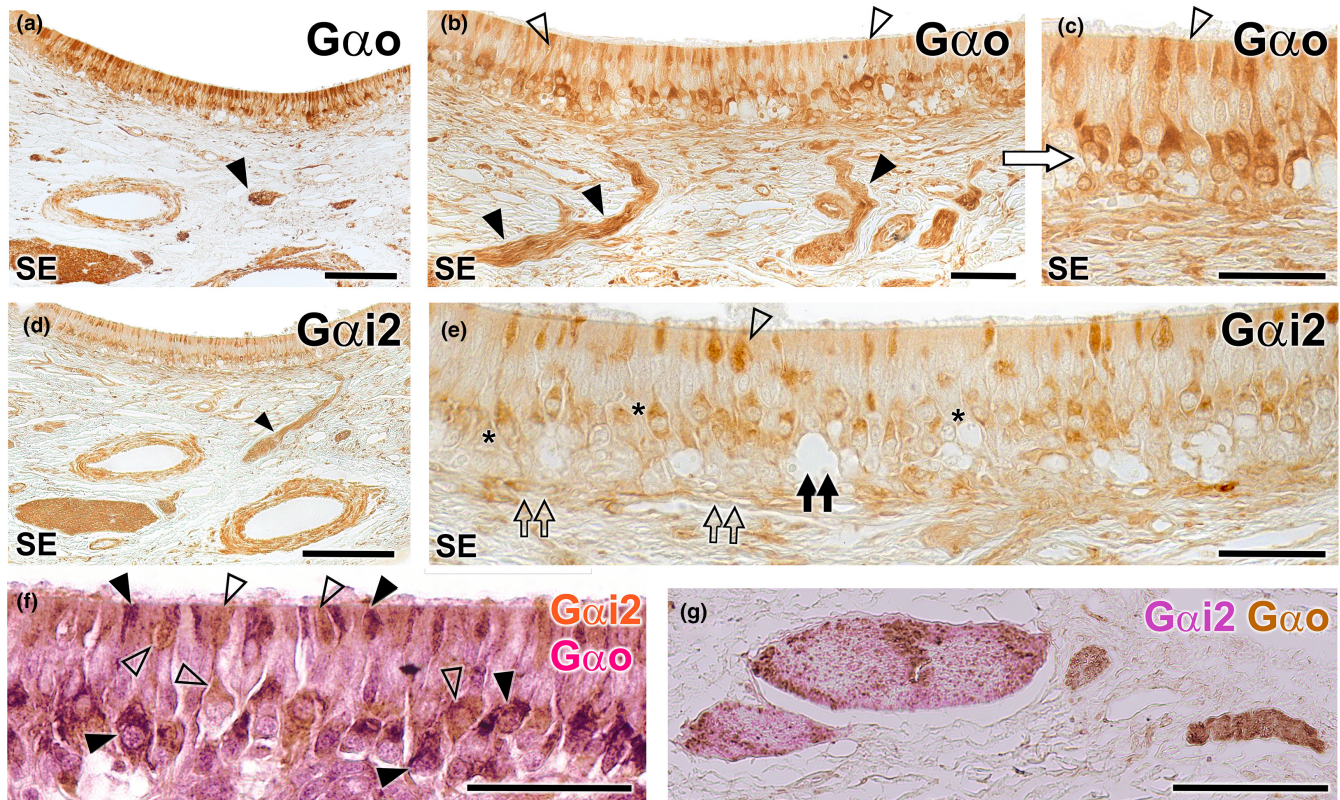
FIGURE 16 Immunohistochemical study of the wolf VNO. Gαo (a–c): Immunolabelling with anti-Gαo shows a pattern of neuronal labelling predominantly concentrated in the neuroreceptor cells present in the basal layers of the neuroepithelium (a and b) and extending to the adjacent vomeronasal nerves (arrowheads). At higher magnification (c: enlarged area of the blue box in image b), it is appreciated how the labelling extends along the entire length of the immunopositive neuroreceptor cells, from the apical dendrite (open arrowhead) to the soma. Immunopositive neuroreceptor cells embrace the intraepithelial capillaries of the VNO. Gαi2 (d, e): The labelling is predominantly concentrated in the neuroreceptor cells mainly located in the central zone of the epithelium (asterisk) and the vomeronasal nerves (arrowhead). Unlike Gαo, no immunopositive neurons are identified around the intraepithelial capillaries (black double arrow). The dendritic knobs are less numerous than in Gαo but more dilated (open arrowhead). The deep neuronal clusters are immunonegative (open double arrows). (f–g): f Double immunostaining for Gαi2 and Gαo confirms the presence of two subpopulations of vomeronasal neuroreceptor cells. Anti-Gαi2 (brown) immunostains a subpopulation of cells predominantly located in the central zones, which have thick dendritic knobs (open arrowheads). Anti-Gαo (red) stains a cell subpopulation mainly located in a more basal zone (black arrowheads). (g) In some cases, as the one shown, the vomeronasal nerves in the parenchyma are predominantly composed either of Gαi2 type fibres (red) or Gαo type fibres (brown). Scale bars: (a, d and g) = 100 μm; (b, c, e and f) = 50 μm.

(Figure 16f). The projection of both subpopulations to the vomeronasal nerve fibres in the parenchyma of the VNO in most cases was not differential, as the nerve branches showed a mixture of both immunolabelling, but in some cases, some nerves showed a differential staining being mostly either Gaio or Gai2 immunopositive (Figure 16g).

The anti-calbindin antibody generates a uniform immunolabeling pattern across the neuroreceptor cell layer, encompassing the vomeronasal nerves (Figure 17a). These immunopositive cells constitute a regularly aligned subpopulation situated in an intermediate area between the basal and apical layers. However, the terminal knobs are poorly labelled, and there is an absence of immunopositivity in the basal clusters (Figure 17b). In contrast, the anti-calretinin antibody demonstrates strong immunopositivity in the basal neuronal clusters (Figure 17c). In addition, a subpopulation of neuroreceptor cells whose dendrites show dilated terminal knobs can be identified. Vomeronasal nerves are also stained.

Anti-OMP, which binds to OMP (a protein serving as a marker of neuronal maturation), produces diffuse labelling throughout the epithelium, including the basal clusters (Figure 18d). Conversely, anti-GAP-43, which binds to GAP43, a protein associated with neuronal axonal growth, presents a similar pattern but lacks labelling of the neuronal clusters (Figure 18e).

3.5 | Histological study of the nasal septum mucosa (Figure 18)

To trace the pathway of the vomeronasal nerves through the nasal septum, we carried out immunohistochemical labelling after dissecting the nasal mucosa, employing antibodies against the G alpha subunit proteins (Figure 18).

While the Gαi2 subunit yielded distinct and specific labelling of the vomeronasal nerves (Figure 18a, a' and a''), the antibody targeting Gαo
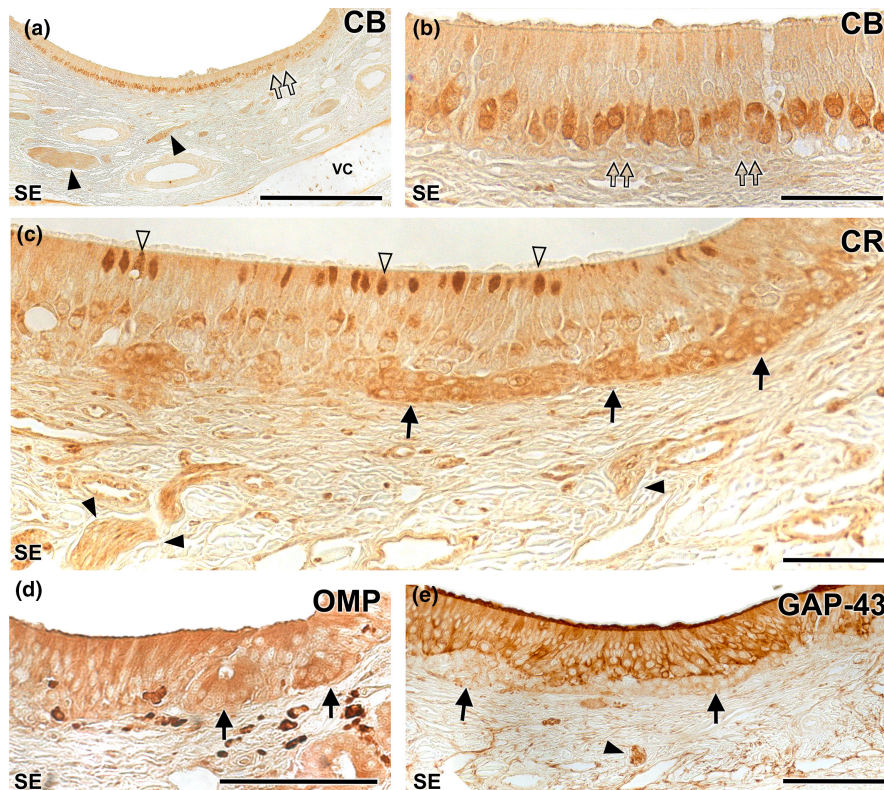
FIGURE 17 Immunohistochemical study of the wolf VNO. Calbindin (CB) (a–b): At low magnification (f) uniform labelling is observed throughout the neuroreceptor cell layer, extending into the vomeronasal nerves (black arrowheads). No immunopositivity is observed in the clusters (double arrows). At higher magnification (g: magnification of the blue box in f) how the immunopositive cells correspond to a regularly aligned subpopulation in an intermediate zone between the basal and apical layers is appreciated. The terminal knobs are poorly labelled. Calretinin (CR) (c): A strong immunopositivity to the neuronal clusters is observed (arrows). In addition, a subpopulation of neuroreceptor cells whose dendrites show dilated terminal knobs can be identified (white arrowheads). Vomeronasal nerves (black arrowhead). OMP (d): Anti-OMP produces a diffuse labelling throughout the epithelium, including the basal clusters (arrows). GAP-43 (e): Pattern similar to (i) but without labelling the neuronal clusters (arrows). Arrowhead: vomeronasal nerves. SE: Neurosensory epithelium. VC: Vomeronasal cartilage. Scale bars: (a) = 250 μm; (d and e) = 100 μm; (b and c) = 50 μm.

not only stained the vomeronasal nerves but also the olfactory nerves coursing through the mucosa of the nasal cavity and the olfactory neuroepithelium from which these axons originate (Figure 18b, b' and b″).

3.6 | Histological analysis of the AOB (Figure 19)

We examined the histological structure of the AOB using haematoxylin and eosin staining (Figure 19a–c,f) and Nissl staining (Figure 19d,e,g,h), both performed on serial sagittal sections. Both stains revealed a significant development of this structure, particularly in relation to its two superficial layers: the nerve layer and the glomerular layer (Figure 19a–e). The nerve layer represents the arrival point for the vomeronasal nerves (Figure 19f,g), while the glomerular layer consists of well-defined, broad and rounded glomeruli that are clearly visible with both stains (Figure 19f,g). The mitral cells are diffusely distributed in a wide zone located between the glomerular layer and the granular layer, thereby precluding the distinction between true plexiform and mitral layers. As a result, the term 'mitral-plexiform layer' (MPL) is employed to describe this region (Figure 19e,h). The granular layer contains

clusters of small, rounded cells interspersed within the white matter (Figure 19h).

3.7 | Immunohistochemical study of the AOB (Figure 20)

The immunohistochemical examination of the wolf AOB using antibodies targeting G protein subunits produced complementary labelling patterns for both Gαi2 and Gαo subunits. Anti-Gαi2 presented uniform and intense immunostaining in the superficial nervous and glomerular layers of the AOB layers (Figure 20a). In contrast, anti-Gαo produced a reverse pattern, with strong immunopositivity observed in the neuropil surrounding the AOB's superficial layers. Both the mitral-plexiform and granular layers of the AOB were immunostained with anti-Gαo. However, the superficial layers were immunonegative, although some immunopositive punctae areas were observed (Figure 20b). These immunolabeling patterns correspond to the dendritic projections of mitral cells within the glomerular layer. Furthermore, calcium-binding proteins such as calbindin (Figure 20c) and calretinin (Figure 20d), as well as OMP (Figure 20e),
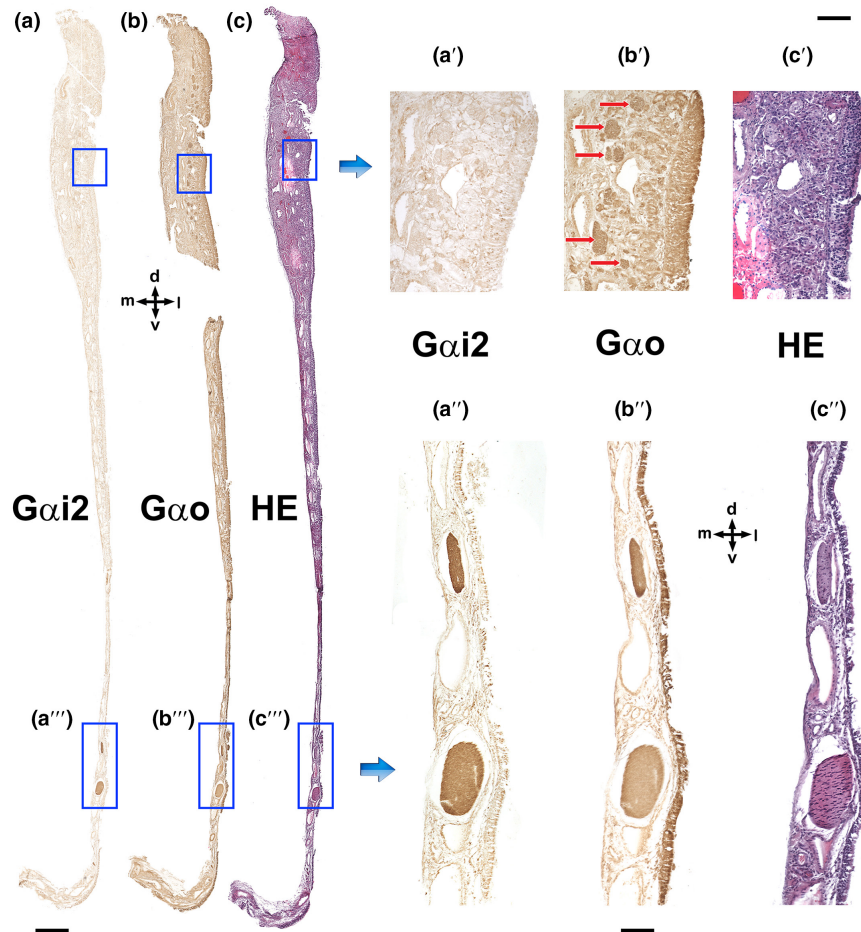
FIGURE 18 Immunolabelling of the VNO nasal septum mucosa with anti-G proteins subunits. (a) Anti-Gαi2 exclusively stains the vomeronasal nerves as they run through the mucosa of the nasal septum (a"). Therefore, anti-Gαi2 does not produce positive immunolabelling of the olfactory nerves, which run in the upper part of the olfactory mucosa (a'). (b) Anti-Gαo (b) stains both the vomeronasal nerves (b") and the olfactory nerves in the mucosa (b', red arrows). (c) Haematoxylin–eosin adjacent section. d, Dorsal; l, lateral; m, medial; and v, ventral. Scale bars: (a–c) = 500 μm; (a'–c' and a"–c") = 100 μm.

showed an identical labelling pattern to that obtained with anti-Gαi2, with the immunolabeling concentrated in both the superficial layers, contrasting with an immunonegative neuropil.

The use of anti-GFAP, a specific marker for glial cells, resulted in a trabecular labelling pattern in the nerve and glomerular layers, which corresponded to the ensheathing glia accompanying the vomeronasal nerve endings (Figure 20f). Occasionally, cell bodies belonging to these glial cells were visible (Figure 20i). Meanwhile, anti-MAP2, a reliable marker for the somata and dendritic projections of the principal cells in the olfactory bulb, exhibited strong labelling within an irregular band corresponding to the MPL layer (Figure 20g). MAP-2 immunopositive prolongations originating from the MPL could be observed running between the glomeruli of the AOB (Figure 20h).

3.8 | Lectin histochemical study of the AOB (Figure 21)

Both lectins employed labelled the AOB. On the one hand, UEA lectin specifically labelled the superficial layers of the AOB (Figure 21a),

while the entire surrounding neuropil remained negative. On the other hand, LEA lectin produced a labelling pattern similar to UEA, with strong labelling in the AOB's superficial layers, making it challenging to differentiate between the nervous and glomerular layers (Figure 21b). The surrounding neuropil showed a diffuse labelling pattern.

4 | DISCUSSION

Chemical communication, facilitated by pheromones, has long been recognised as an essential component of social and sexual interactions among canids. These complex chemical signals are detected and processed by the VNS, serving a range of functions from mate selection and social hierarchy establishment to territory marking. They are also integral to the reproductive physiology of these animals (Gorman & Trowbridge, 1989).

In this study, we aimed to contribute to the ongoing research on the neuroanatomical and neurochemical aspects of the VNS in canids. Specifically, we focus on the Iberian wolf (*Canis lupus signatus*), an emblematic species of great ecological importance and cultural
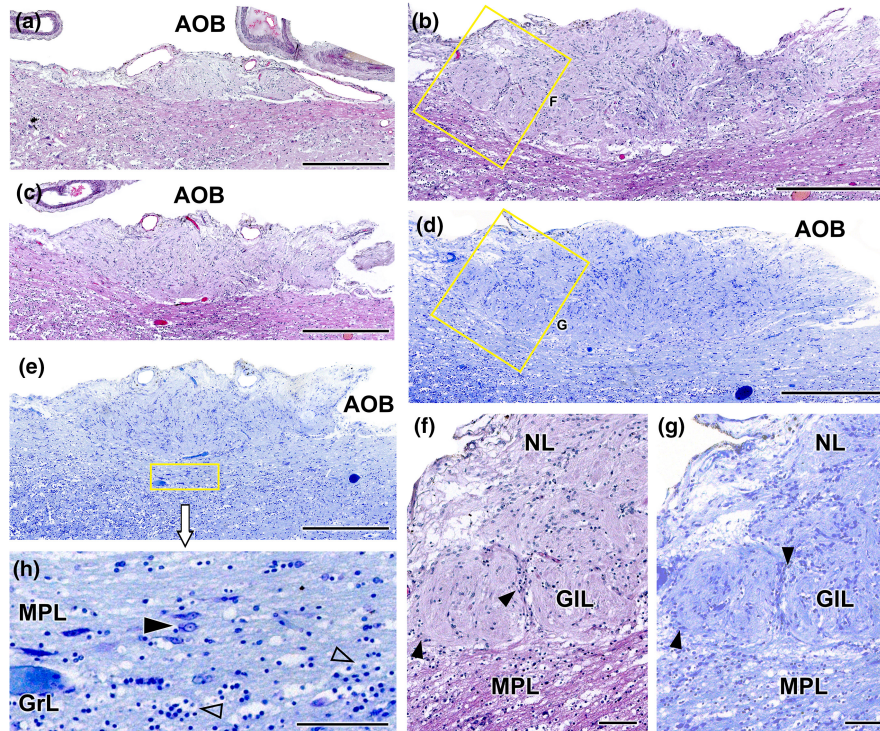
FIGURE 19 Histological study of the wolf accessory olfactory bulb stained with haematoxylin–eosin and Nissl staining. (a–c). A general view of the AOB can be seen at three selected sagittal levels stained with HE. They show the elongated shape of this structure and the predominance of the nervous (NL) and glomerular layers (GIL). (d, e) Sagittal Nissl-stained sections at low magnification allows to appreciate the development of the AOB. (f) At higher magnification (corresponding to box in b), two glomerular formations clearly defined by periglomerular cells (arrowheads) are appreciated. (g) The magnification of the superficial area of the AOB (box in d) allows to discriminate the presence of a mitral-plexiform layer (MPL). (h) Enlargement of the deep area of the AOB (corresponding to box in e) shows mitral cells (black arrowhead) in the MPL as well as granular cells (open arrowhead) in the deeper granular layer (GrL). Scale bars: (a–e) = 500 μm; (f–h) = 100 μm.

significance, with a crucial role in ecosystem dynamics. Surprisingly, up to this point, there has been limited exploration of the neuro-anatomical features of its VNS. Notably, research on VNS in domestic dogs has witnessed substantial growth in the past decade, highlighting its crucial role in shaping the socio-sexual behaviours of domestic canines (Muñiz-de Miguel et al., 2023), as well as its potential involvement in pathological conditions leading to significant behavioural changes (Asproni et al., 2016). Consequently, clinical interest in this sensory system has considerably increased (Dzięcioł et al., 2020; Pageat & Gaultier, 2003).

Conversely, a primary limitation in the existing literature is the paucity of research pertaining to wild or feral canids. There are only a few notable exceptions, such as the study by Chengetanai et al. (2020), who investigated the neuroanatomy of the African wild dog's AOB as part of their broader investigation of the olfactory system in this species. Recent studies on foxes have unveiled considerable anatomical and functional differences when comparing these wild foxes to their domestic counterparts. Remarkably, these fox studies have identified specific features in the structure and neurochemistry of the VNO (Ortiz-Leal et al., 2020), AOB (Ortiz-Leal, Torres, Villamayor, et al., 2022) and the transitional zone commonly referred to as the olfactory limbus (Ortiz-Leal et al., 2023).

In the subsequent sections, we focus on the key findings of our research, with a specific focus on the unique neuroanatomical features of the VNS in wolves and its evolutionary implications. To achieve this, we not only compare our data with the extensively researched VNS of the domestic dog but also incorporate available data on other wild canid species. Additionally, our goal is to contextualise our results within the larger framework of carnivorous taxa, with a particular emphasis on felids, mustelids and ursids. This approach will help elucidate the adaptive, evolutionary or potentially convergent characteristics of these chemosensory systems. In essence, this study seeks to provide a neuroanatomical basis for guiding future investigations into the chemical ecology of not only wild canids but also other carnivorous taxa.

4.1 | VNO macroscopic study

We employed both cross sectional macroscopic anatomy and CT scans to meticulously delineate the topographic relationships and macroscopic features of the wolf's VNO. The use of CT scans to characterise VNO anatomy has been relatively limited, with only a small number of studies dedicated to this specific area. Previous research has been largely restricted to goats (Moawad et al., 2017),
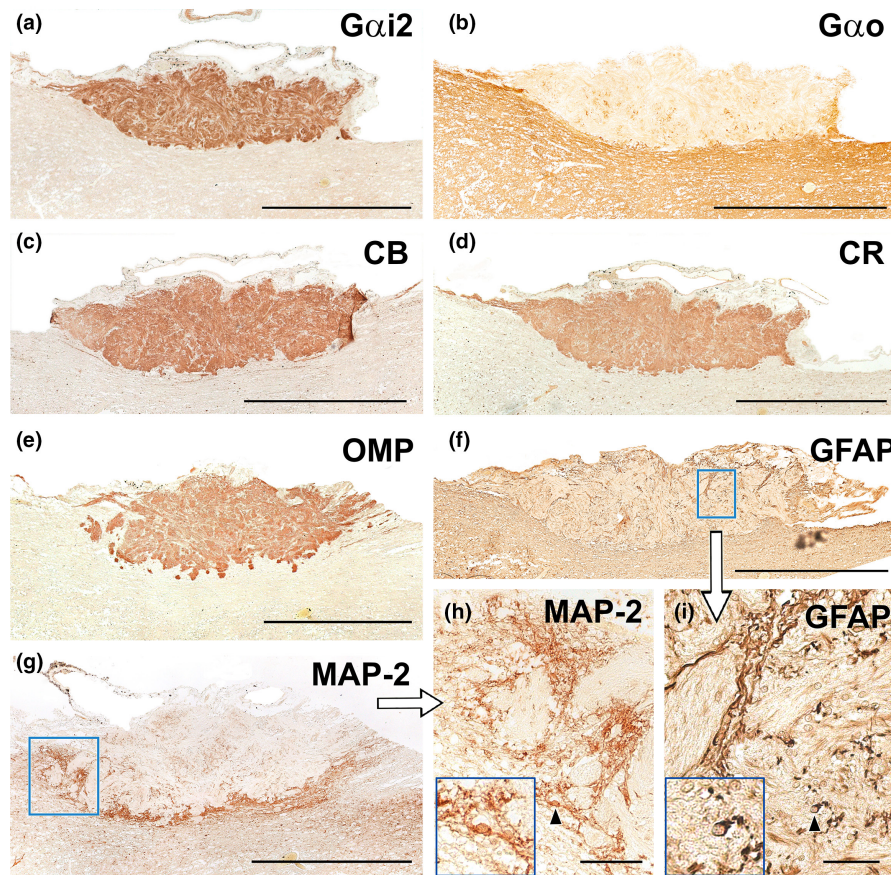
FIGURE 20 Immunohistochemical study of wolf AOB. (a) Anti-Gαi2 uniformly and intensely label the superficial layers of the AOB (nervous and glomerular layers). The entire surrounding neuropil is negative. (b) Anti-Gαo produces a reverse pattern to the one shown in A, where the neuropil surrounding the superficial layers is strongly immunopositive, including the mitral-plexiform and granular layers of the AOB. However, the superficial layer is clearly negative, although immunopositive punctae areas are observed. (c–e) The calcium binding proteins, calbindin (c) and calretinin (d), as well as OMP (e) show an identical labelling pattern to that obtained with anti-Gαi2, concentrated in both the nerve and glomerular layers and immunonegative for the neuropil. (f) Anti-GFAP (f and enlarged area in i) produces a trabecular labelling pattern in the nerve and glomerular layers, which corresponds to the ensheathing glia accompanying the vomeronasal nerve endings. Occasionally, cell bodies belonging to these glial cells are visible (arrowhead). The cell body is magnified in the bottom left-hand box. (g) Anti-MAP-2 immunolabelling does not produce immunopositive labelling in the superficial layers (nervous and glomerular), but it strongly labels an irregular band corresponding to the MPL layer. (h) MAP-2-immunopositive prolongations originating from the MPL can be observed running between the glomeruli of the AOB. (h: enlargement of the box in g). The cell body of an immunopositive interneuron (arrowhead) is shown in an enlarged view in the box at the bottom left. Scale bars: (a–g)=500μm; (h–i)=50μm.

camels (Alsafy et al., 2014), bats (Yohe et al., 2018) and mice (Levy et al., 2020; Mucignat, 2004). In the case of mice, researchers have employed high-resolution magnetic resonance and micro-CT techniques in their studies. Our results corroborate the bilateral positioning of the wolf's VNO in the most rostral and ventral regions of the nasal cavity. It is situated laterally to the vomer bone and ventrally to the cartilage of the nasal septum, predominantly occupying the internal side of the palatine fissure. Our serial anatomical sections illustrate how the VNO is highly adapted to the contours of the nasal cavity, reinforcing the notion that its strategic placement may optimise its functional efficacy. This positioning facilitates communication through the ID, connecting the organ to the external environment through both the nasal and oral cavities. This suggests a complex interplay between these two cavities, potentially enabling a multi-modal sensory input for the wolf.

Given its intricate location and the complete covering of the cartilaginous capsule of the VNO by the nasal cavity's respiratory mucosa, visualising the organ proves challenging both in vivo and post-mortem. The presence of the caudal nasal myelinated nerve at the most caudal extremity of the VNO serves as a reliable indicator of its location. Additionally, the vomeronasal nerve fibres were observed to run in a caudodorsal direction, indicating an integrated neuroanatomical pathway with the MOS. The cartilaginous capsule almost entirely envelopes the parenchyma of the VNO, except for its dorsolateral part. This pattern is similar to those described in other carnivores such as dogs (Salazar et al., 2013), foxes (Ortiz-Leal et al., 2020), ferrets (Kelliher et al., 2001), minks (Salazar, Cifuentes, Quinteiro, & Caballero, 1994) and bears (Tomiyasu et al., 2017). However, it is somewhat less extensive compared to the complete encapsulation observed in felines (Salazar et al., 1995). While our
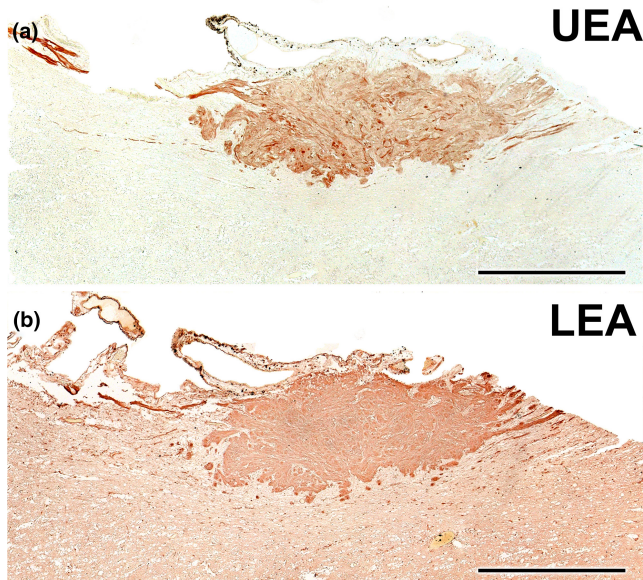
FIGURE 21 Lectin histochemical study of the wolf AOB. (a) UEA lectin labels uniformly and strongly the superficial layers of the AOB (nervous and glomerular layers). The entire surrounding neuropil is negative. (b) LEA-lectin produces a similar labelling to UEA but with higher intensity in the AOB superficial layers and a diffuse pattern in the surrounding neuropil. Scale bar = 500 μm.

macroscopic study primarily had an anatomical focus, our observations have functional implications. For instance, the VNO's location adjacent to the root of the upper canine tooth suggests a potentially critical role in sensing pheromones during aggressive or mating behaviours.

4.2 | VNO's histological features

Our histological analysis of the VNO reveals a complex microanatomy essential for understanding its potential physiological and behavioural functions. The U-shaped cartilaginous structure that encapsulates the soft tissue serves a crucial role: It prevents the soft tissue from collapsing under the negative pressure generated by the vomeronasal pumping mechanism designed to intake pheromones (Meredith, 1994; Meredith et al., 1980; Meredith & O'Connell, 1979). The presence of a complex venous network within the wolf VNO is a noteworthy finding. Notably, our examination reveals a complex venous network within the wolf's VNO. Although this feature is also characteristic of the VNO in dogs and cats, as reported by Salazar et al. (1997, 2013), all the wolf specimens we studied presented a more advanced development of the vascular component. This is particularly evident in the predominance of large, muscular veins located in the dorsal and lateral regions of the organ. This venous preponderance plays a crucial role in the functioning of the vascular pump. When these vascular structures within the soft tissue contract, the lumen of the vomeronasal duct expands, creating a vacuum effect that draws in chemical molecules. Conversely, vascular dilation causes the duct

to constrict, leading to the expulsion of its contents, as described by Eccles (1982).

The limited presence and reduced size of arteries in the VNO may suggest that the organ does not require a high supply of oxygenated blood for its primary function of chemoreception. This could imply an energy-efficient mechanism, where the organ operates optimally without needing substantial blood flow, possibly reflecting evolutionary adaptations that prioritise efficiency in sensory organs (Niven & Laughlin, 2008).

Further, our observations of blood capillaries in the neuroepithelium of the organ suggest the presence of mechanisms that enhance the efficiency of nutrient and gas supply to the VNO. Interestingly, these capillaries are in direct contact with the neuroreceptor layer, raising speculation about the possibility of haematogenic olfaction (Bednar & Langfelder, 1930). Although this olfactory paradigm is not definitively proven, recent findings indicating that the VNO serves as a critical sensor for haemoglobin in rodents (Osakada et al., 2022) support this hypothesis. Intraepithelial capillaries have previously been characterised in rats (Breipohl et al., 1981), a species with a notably thick epithelium requiring substantial blood supply. In contrast, intra-epithelial blood vessels have not been reported in species with neuroepithelium composed of only a few cell rows, such as lemurs (Smith et al., 2007, 2015), tree shrews, slow lorises (Loo & Kanagasunteram, 1972), certain primates (Smith, Garrett, et al., 2011) and bats (Bhatnagar & Meisami, 1998; Bhatnagar & Smith, 2007). The presence of these intra-epithelial capillaries in wolves, a species with significantly fewer neuroreceptor cells compared to rodents, is quite striking. To our current understanding, no descriptions of the dog VNO refer to the presence of such intra-epithelial capillaries (Dennis et al., 2003; Salazar et al., 2013). This could represent a significant morphological distinction that may have implications for the functional capabilities of the VNO in these closely related species.

The interaction of the vomeronasal duct with the external environment demonstrates notable similarities between our findings on decalcified histological series in wolves and what has been described in dogs (Adams & Wiekamp, 1984; Salazar et al., 2013). This indirect interaction involving the ID is also evident in other carnivores such as foxes (Ortiz-Leal et al., 2020), minks (Salazar, Cifuentes, Quinteiro, & Caballero, 1994) and bears (Tomiyasu et al., 2017), as well as in mammals from other orders including cows (Jacobs et al., 1981), moose (Vedin et al., 2010) and hedgehogs (Kondoh et al., 2021). One end of the ID communicates with the vomeronasal duct through the ventral recess of the nasal cavity, while its other end connects to the oral cavity via the incisive papilla. This distinct anatomical configuration distinguishes these species from rodents and lagomorphs. In the latter group, the vomeronasal duct directly opens into the nasal cavity, and the ID serves as an independent link between both cavities (Vaccarezza et al., 1981; Villamayor et al., 2018).

The relatively sparse glandular tissue, concentrated near the ventral and particularly the dorsal commissures, appears to play a specialised role in either secretion or absorption, thereby maintaining a continuous mucous environment within the vomeronasal duct

(Halpern & Martínez-Marcos, 2003). In wolves, as in dogs (Kondoh et al., 2020) and foxes (Ortiz-Leal et al., 2020), a few glands are observed in the central and medial portions of the organ, with their numbers increasing progressively towards the caudal portions. Using Alcian Blue stain, we were able to characterise the nature of the glandular secretions in the wolf's VNO as AB-positive. The presence of AB-positive vomeronasal glands has also been observed in foxes (Ortiz-Leal et al., 2020). In contrast, Kondoh et al. (2020) reported that vomeronasal glands in dogs were solely PAS-positive. In the case of other carnivore species, Tomiyasu et al. (2018) identified both PAS- and AB-positive glands in bears. Meanwhile Salazar et al. (1996) and Kondoh et al. (2020) identified only PAS-positive glands in cats and dogs respectively. These variations may be attributed to the specific region of the VNO under examination, as most studies have primarily focused on its central region, where we have observed a lower glandular tissue density. Future investigations that examine the nature of vomeronasal gland secretion along the entire axis of the dog's VNO are expected to provide further insights into this matter.

The organisation of the vomeronasal, sensory and respiratory epithelia essentially follows the pattern described in other canids such as dogs (Salazar, Cifuentes, Sánchez Quinteiro, & García Caballero, 1994) and foxes (Ortiz-Leal et al., 2020), except for the notable presence of conspicuous cellular clusters in a basal position (Figure 9b). These cellular accumulations, due to their density and the size of the cells composing them, are clearly distinct from the layer of basal cells and the neuroreceptor cells. Moreover, as will be discussed later in the text, the immunohistochemical study shows that they present a unique pattern of immunostaining. Other histological features of the wolf's VNO closely resemble the information available on dogs. Specifically, the abundant connective tissue found throughout the wolf's VNO likely plays a vital role in maintaining structural integrity. This tissue acts as a scaffold, preserving the intricate microanatomy essential for the specialised functions of the VNO (Takami, 2002). Additionally, the identification of two distinct types of nerve fibres in the VNO—myelinated and unmyelinated—is a shared feature between both species. These fibre types are, respectively, related to sensory perception and the autonomic control of blood vessels and glands (Iwanaga & Nio-Kobayashi, 2020).

4.3 | VNO's immunohistochemical features

The immunohistochemical characterisation of the wolf VNO reveals distinctive expression patterns for various G protein subunits and neural markers, including calbindin, calretinin, OMP and GAP-43. These markers serve as indicators for various functional roles and developmental stages within the VNO's neuroreceptor cells.

Of particular importance is the immunohistochemical analysis employing specific antibodies targeting the alpha subunits of Gi2 and Go proteins. This significance is reinforced by both neurochemical (Shinohara et al., 1992) and genomic studies (Dulac &

Axel, 1995; Herrada & Dulac, 1997; Matsunami & Buck, 1997; Ryba & Tirindelli, 1997) in rodents, which consistently associate the Gαi2 protein with the expression of the V1Rs receptor family in the VNS, whereas the Gαo protein is linked to the V2Rs family. Subsequent research has revealed the absence of the Gαo pathway in various mammals, including both Laurasiatheria and Primates (Suárez, Fernández-Aburto, et al., 2011; Takigami et al., 2000). Nevertheless, studies focusing on G protein expression in the VNS of Carnivora have been a point of debate.

Initially, Dennis et al. (2003) reported immunopositive labelling in the dog VNO neurosensory epithelium using both anti-Gαi2 and anti-Gαo antibodies, suggesting an unintended consequence of the antigen retrieval process. This theory gained further credence in a later study by Salazar et al. (2013), who reported immunonegative labelling using the anti-Gαo antibody when antigen retrieval was not applied. However, more recent discoveries confirmed the presence of Gαo protein immunoreactivity in the fox's VNO neuroepithelium (Ortiz-Leal et al., 2020) and the vomeronasal nerves in the nasal mucosa and cribriform plate (Ortiz-Leal, Torres, Villamayor, et al., 2022). This unexpected expression pattern in the fox has now also been confirmed in another wild canid, the wolf. Specifically, the anti-Gαo antibody predominantly labelled neurons located in the basal layers of the vomeronasal neuroepithelium. These marked cells were in proximity to intra-epithelial capillaries, suggesting their potential involvement in vascular interactions or haematogenic olfaction. In contrast, the cells labelled by the anti-Gαi2 antibody were situated in the central zone of the epithelium and exhibited no discernible association with intra-epithelial capillaries. The performance of double immunohistochemical labelling against both G proteins subunits allowed for an accurate verification of the presence of both neuroreceptor cells subpopulations, as both markers enabled a clear differentiation of two cell subpopulations, both at the level of neuronal somas and dendritic buttons. This differentiation in some cases extended to the branches of vomeronasal bundles in the parenchyma of the VNO.

While the immunohistochemical identification of Gαo is often regarded as a reliable marker for V2R expression in the VNO, this notion is not fully corroborated by existing genomic studies. These studies suggest that functional V2R genes have become vestigial in numerous mammalian groups, including carnivores, through accelerated pseudogenisation (Young & Trask, 2007). However, translating genomic findings into neuroanatomical facts presents challenges because of the mismatch between genetic and morphological aspects in chemosensory systems. To bridge this gap, further morphological investigation is essential, particularly focusing on the associated brain regions, glands and ducts (Yohe & Krell, 2023). The prevalence of pseudogenes among vomeronasal receptors prompts inquiries and may explain the discrepancy between sequencing data and anatomical observations. This complexity is exemplified by an olfactory receptor gene that, despite having a premature stop codon, encodes a functional protein through efficient translational readthrough (Prieto-Godino et al., 2016; Stensmyr, 2016). Additionally,

transcriptomic studies have identified the expression of vomeronasal pseudogenes within the mouse's VNO (Dietschi et al., 2022; Oboti et al., 2015).

The notion that the Gαo protein may play a role in cell-to-cell signalling within the wolf neuroepithelium remains a possibility. However, such a role in the mammalian vomeronasal neuroepithelium has not been confirmed. Moreover, this hypothesis does not align with the Gαo immunolabeling pattern in the wolf's VNO, which extend through dendritic processes, cell bodies and axons forming the vomeronasal nerves—a pattern that is consistent with both G proteins being involved in transduction mechanisms (Mohrhardt et al., 2018).

The presence of both Gαi2 and Gαo proteins in the sensory epithelia of the wolf's and fox's VNO diverges from the isolated expression of Gαi2 protein in other carnivores like dogs and cats (Salazar et al., 2013; Salazar & Sánchez-Quinteiro, 2011). This raises intriguing questions about the impact of domestication. The absence of Gαo protein expression in the VNS of domestic animals, such as goats (Takigami et al., 2000), sheep (Salazar et al., 2007), dogs (Salazar et al., 2013) and cats (Salazar & Sánchez-Quinteiro, 2011) has led to the hypothesis that domestication may have contributed to the degeneration of the VNS (Jezierski et al., 2016).

A range of supplementary antibodies, including anti-CB, anti-CR, anti-GAP-43 and anti-OMP, were employed for the immunohistochemical examination of the VNO. The anti-CB and anti-CR antibodies are frequently used to characterise neuronal subpopulations, revealing unique expression profiles in the VNS across diverse species (Bastianelli & Pochet, 1995; Briñón et al., 2001; Malz et al., 2000). In the case of wolves, the anti-CB antibody demonstrated a distinct immunolabeling pattern within the sensory epithelium, highlighting a subset of neuroreceptor cells predominantly located in the deeper layers of the epithelium. The labelling was the most concentrated in the cell bodies and less so in the dendritic extensions. Conversely, the anti-CR antibody produced labelling that complemented that of the anti-CB antibody, targeting somata located more superficially within the epithelial layer. Notably, the dendritic buttons on these neurons appeared bulb-shaped and were strongly stained.

The anti-GAP43 antibody, employed to identify neurons undergoing axonal development and synaptogenesis (Gispen et al., 1991; Ramakers et al., 1992; Verhaagen et al., 1989), showed an intense and widespread labelling pattern. This pattern remained consistent with findings observed in both foxes (Ortiz-Leal et al., 2020) and dogs (Dennis et al., 2003), suggesting an active process of neuronal regeneration within the canine vomeronasal sensory epithelium. This ongoing plasticity could be in response to the VNO's frequent exposure to various environmental substances with the potential to cause cellular damage (Ogura et al., 2010). These observations underscore the significance of the vomeronasal sensory system in canids.

Finally, the anti-OMP antibody targeted the olfactory marker protein, which is expressed in mature neurons within both the MOS and the VNS (Farbman & Margolis, 1980). It has shown immunopositive labelling in a range of species, including rats (Rodewald et al., 2016), mice (Mechin et al., 2021), mole rats (Dennis et al., 2020) and primates (Smith, Dennis, et al., 2011). The ubiquitous presence of OMP within the wolf's VNO suggests a uniform stage of neuronal maturation throughout the epithelium.

Beyond the intricate neurochemical pattern observed in the sensory neuroepithelium of the wolf's VNO—an indication of the complex interplay of molecular and cellular communication and signal transduction mechanisms involved in pheromonal information processing—our immunohistochemical study has identified a striking, distinctive feature of the wolf's VNO. This feature consists of abundant clusters of neuronal cells situated in the most basal part of the sensory neuroepithelium (Figure 9b). These clusters extend for several hundred micrometres immediately beneath the basal layer of neuroreceptor cells (Figures 15a,d,e and 17c–e). They comprise oval-shaped cells with large spherical nuclei, densely packed and seemingly devoid of processes. While their morphology may superficially resemble that of the neuroreceptor cells in the neuroepithelium, these cells display a specific neurochemical pattern. On the one hand, these cells are OMP-positive, reinforcing their role in olfactory signal transduction. On the other hand, they are immunonegative for GAP-43, suggesting a state of higher differentiation compared to the highly GAP-43-positive neuroreceptor cells. These observations do not align with the notion that these are undifferentiated cells serving to renew the epithelium, akin to typical basal cells. Regarding calcium-binding proteins, these clusters are calretinin-positive and calbindin-negative, which could initially establish a link between them and the calretinin-positive cell subpopulation.

The presence of these clusters is seemingly specific to the wolf's VNO. Our comprehensive study of the fox VNO (Ortiz-Leal et al., 2020), using similar markers and protocols, did not reveal a similar neuroepithelial organisation. Furthermore, studies on other carnivores such as dogs, minks, ferrets and bears have not yielded comparable findings. Despite decades of research on the VNO in a diverse array of mammals, this unique neuroepithelial organisation has neither been encountered by us in our studies (Torres, Ortiz-Leal, & Sanchez-Quinteiro, 2023) nor, to the best of our knowledge, has it been reported by other researchers. This suggests that such an organisation may represent a specialised evolutionary adaptation unique to this species, the wolf.

Hypothetically, clusters of neurons beneath the vomeronasal epithelium in the lamina propria, distinct from the vomeronasal neuroreceptor cells, could serve various functions. Its position in the lamina propria would enable the rapid detection of molecules in the surrounding blood vessels, facilitating the response of the epithelium to these changes. The clusters might as well modulate pheromonal signals, regulating signal intensity or quality before reaching central processing areas. Alternatively, they might respond to specific non-pheromonal stimuli, playing a role in alert or defensive functions. Additionally, these clusters might be linked to tissue homeostasis, detecting and responding to environmental changes in the local surroundings. Lastly, they could act as relay stations, transmitting signals to specific brain areas beyond the vomeronasal

epithelium. These hypotheses are speculative and would require further research for validation.

Therefore, further specialised research into these cell clusters, employing additional markers, or even genomic approaches such as RNAscope or single-cell technology, is imperative to more comprehensively characterise this distinctive cell population. This approach will enhance our understanding of its functional role and significance within the VNO.

4.4 | VNO lectin histochemical labelling

Our lectin histochemical investigation reveals subtle differences in the labelling patterns of UEA and LEA lectins within the VNO sensory epithelium and vomeronasal nerves. Both lectins produce positive labelling in neuroreceptor cells and the vomeronasal nerves; yet, they diverge significantly when it comes to the basal neuroepithelial cell clusters. LEA labels these neuronal clusters, whereas UEA does not, suggesting distinct molecular interactions between these lectins and the cellular components of the clusters. Furthermore, LEA shows stronger labelling in the apical processes, while UEA is more concentrated in basal areas of the epithelium, although it never labels the basal clusters.

In the respiratory epithelium, both lectins manifest diffuse but specific labelling patterns. LEA primarily targets the apical processes, whereas UEA labelling is sparser, with a few strongly labelled cells dispersed throughout the epithelium. Within the mucociliary complex, UEA shows stronger labelling compared to LEA. These distinct labelling patterns suggest that the glycoconjugates recognised by these lectins possess specialised molecular functions within the VNO.

4.5 | AOB macroscopic and microscopic anatomy

To the best of our knowledge, this study represents a pioneering morphological investigation of the wolf's AOB. Similar to other studied canids, such as the dog (Nakajima et al., 1998; Salazar & Sánchez-Quinteiro, 2011), the African wild dog (Chengetanai et al., 2020) and the fox (Ortiz-Leal, Torres, Villamayor, et al., 2022), the wolf's AOB is considerably smaller in size compared to the MOB, rendering its macroscopic identification challenging. Accurate localisation of this structure necessitates the use of serial histological sections. The study of the cytoarchitecture of the wolf's AOB is particularly pertinent, given the historical debate surrounding the moderate development, and even the very existence, of the AOB in dogs. This controversy was only resolved in the 1990s with the advent of lectin histochemical staining techniques (Salazar et al., 1992; Salazar, Cifuentes, Sánchez Quinteiro, & García Caballero, 1994).

Our research confirms the existence of an AOB in the wolf, with dimensions comparable to those found in domestic dogs. However, the wolf's AOB exhibits a more pronounced laminar organisation. Notably, there is substantial development in the superficial nervous and glomerular layers of the AOB, along with a higher number of mitral cells, a principal cell type rarely observed in histological sections of the dog's AOB. As a result, the wolf's AOB can be described as possessing a well-defined mitral-plexiform layer. Our findings are in keeping with those of a comprehensive study of the African wild dog's olfactory system, which included an examination of the AOB (Chengetanai et al., 2020). While the size and development of the AOB in wild canids may appear limited, it remains more differentiated than in other groups of carnivores. Specifically, Mustelidae such as the mink (Salazar et al., 1998) and ferret (Kelliher et al., 2001), as well as Herpestidae like the meerkat (Torres et al., 2021), possess poorly differentiated AOBs. Altogether, this morphological research corroborates the presence of distinct lamination patterns in the AOB across wild canid populations and supports the theory that the selection pressure linked to domestication may have regressed the degree of differentiation in the dog's vomeronasal system, a sensory pathway crucial for survival in the wild.

4.6 | AOB immunohistochemistry and lectin histochemistry

The neurochemical profile of the wolf's AOB in its superficial, nervous and glomerular layers mirrors what is observed in the VNO. Proteins, such as Gαi2, CB, CR and OMP, expressed in the vomeronasal neuroepithelium and vomeronasal nerves both in the VNO and the nasal mucosa, are also detected in the superficial layers of the AOB, where they produce immunopositive labelling. However, the superficial layers are Gαo negative. This implies that Gαo-positive vomeronasal neuroreceptors project their information to different areas of the olfactory bulb, a pattern identical to that observed in the VNS of the fox (Ortiz-Leal, Torres, Villamayor, et al., 2022). A recent study on the fox suggested that Gαo vomeronasal afferents project to the olfactory limbus, a transition zone (Ortiz-Leal et al., 2023). The existence of a similar olfactory limbus in the wolf is a subject warranting investigation, as it lies beyond the scope of this study. Of all the markers described in our study, Chengetanai et al.'s (2020) study of the African wild dog's AOB only employed anti-CR, obtaining a pattern similar to the one described by us in the wolf. Similar to the African wild dog, in the wolf, there is no discrimination of calretinin-positive neuronal cells, which contrasts with what is observed in species such as the fox, the mouse or the rabbit, where neuronal staining occurs in the glomerular, mitral-plexiform and granular layers (Jia & Halpern, 2004; Ortiz-Leal et al., 2023; Villamayor et al., 2020). Furthermore, our study of the wolf's AOB used antibodies against MAP-2 and GFAP proteins, enabling us to characterise the remarkable development of the dendritic tree in the mitral-plexiform layer and the glial component, both at the level of the enveloping glia and astrocytes.

Both UEA lectin and LEA produce immunopositivity in the superficial areas of the AOB, but while the former is specific to the AOB, the latter stains both the AOB and the MOB. This pattern is consistent with observations in the dog (Salazar et al., 1992, 2013) and the fox (Ortiz-Leal, Torres, Villamayor, et al., 2022), confirming

the usefulness of UEA as a marker for the VNS of canids and LEA as a general marker for the VNS and MOS in the same family. It is noteworthy, however, that the BSI-B$_4$ lectin, specific to the VNS of the rat (Ichikawa et al., 1992), remains negative in the case of the wolf, demonstrating the remarkably high specificity of glycoconjugate expression across different mammalian groups.

In conclusion, this comprehensive study of the wolf's VNS, encompassing the VNO, vomeronasal nerves and AOB, has provided the first detailed characterisation of its macroscopic anatomy, histology and neurochemical and histochemical profiles. Our findings highlight significant differences between the wolf (*Canis lupus signatus*) and its domestic counterpart, *Canis lupus familiaris*, in terms of both structural and neurochemical aspects. These findings support the hypothesis that the domestication of the dog's ancestor has led to the regression of specific molecular and neurochemical features within the VNS. Beyond its evolutionary implications, it is noteworthy that the wolf's VNS exhibits unique characteristics. It aligns with other animal models presenting the dual expression of G protein subunits in their VNO, a finding of great interest. Particularly remarkable is the presence of extensive neural clusters in the VNO neuroepithelium, previously undocumented in other canid species or any other mammals. This adds new depth to our comparative understanding of the mammalian VNS. Future molecular and genomic investigations are expected to shed light on the significance of these structural and neurochemical features.

AUTHOR CONTRIBUTIONS

I.O.L., M.V.T., T.S. and P.S.Q designed the research and wrote the article. P.S.Q., I.O.L., J.D.B.V., M.V.T., L.F. and A.L.B performed the work. I.O.L., M.V.T., T.S. and P.S.Q analysed and discussed the results.

DATA AVAILABILITY STATEMENT

Date are available under request.

ORCID

Pablo Sanchez-Quinteiro 🄳 https://orcid.org/0000-0002-9891-4817

REFERENCES

Abellán-Álvaro, M., Martínez-García, F., Lanuza, E. & Agustín-Pavón, C. (2022) Inhibition of the medial amygdala disrupts escalated aggression in lactating female mice after repeated exposure to male intruders. *Communications Biology*, 5(1), 980. Available from: https://doi.org/10.1038/s42003-022-03928-2

Adams, D.R. & Wiekamp, M.D. (1984) The canine vomeronasal organ. *Journal of Anatomy*, 138(Pt 4), 771–787.

Alonso, J.R., Briñón, J.G., Crespo, C., Bravo, I.G., Arévalo, R. & Aijón, J. (2001) Chemical organization of the macaque monkey olfactory bulb: II. Calretinin, calbindin D-28k, parvalbumin, and neurocalcin immunoreactivity: calcium-binding proteins in the monkey OB. *Journal of Comparative Neurology*, 432(3), 389–407. Available from: https://doi.org/10.1002/cne.1110

Alsafy, M.A.M., El-gendy, S.A.A. & Abumandour, M.M.A. (2014) Computed tomography and gross anatomical studies on the head of one-humped camel (*Camelus dromedarius*). *The Anatomical Record*, 297(4), 630–642. Available from: https://doi.org/10.1002/ar.22865

Asa, C.S., Mech, L.D., Seal, U.S. & Plotka, E.D. (1990) The influence of social and endocrine factors on urine-marking by captive wolves (*Canis lupus*). *Hormones and Behavior*, 24(4), 497–509. Available from: https://doi.org/10.1016/0018-506X(90)90038-Y

Asproni, P., Cozzi, A., Verin, R., Lafont-Lecuelle, C., Bienboire-Frosini, C., Poli, A. et al. (2016) Pathology and behaviour in feline medicine: investigating the link between vomeronasalitis and aggression. *Journal of Feline Medicine and Surgery*, 18(12), 997–1002. Available from: https://doi.org/10.1177/1098612X15606493

Barja, I., de Miguel, F.J. & Bárcena, F. (2004) The importance of cross-roads in faecal marking behaviour of the wolves (*Canis lupus*). *Naturwissenschaften*, 91(10), 489–492. Available from: https://doi.org/10.1007/s00114-004-0557-1

Barja, I., Silván, G. & Illera, J.C. (2008) Relationships between sex and stress hormone levels in feces and marking behavior in a wild population of Iberian wolves (*Canis lupus signatus*). *Journal of Chemical Ecology*, 34(6), 697–701. Available from: https://doi.org/10.1007/s10886-008-9460-0

Barrios, A.W., Sanchez Quinteiro, P. & Salazar, I. (2014) The nasal cavity of the sheep and its olfactory sensory epithelium. *Microscopy Research and Technique*, 77(12), 1052–1059. Available from: https://doi.org/10.1002/jemt.22436

Barrios, A.W., Sanchez-Quinteiro, P. & Salazar, I. (2014) Dog and mouse: toward a balanced view of the mammalian olfactory system. *Frontiers in Neuroanatomy*, 8, 106. Available from: https://doi.org/10.3389/fnana.2014.00106

Bastianelli, E. & Pochet, R. (1995) Calmodulin, calbindin-D28k, calretinin and neurocalcin in rat olfactory bulb during postnatal development. *Developmental Brain Research*, 87(2), 224–227. Available from: https://doi.org/10.1016/0165-3806(95)00073-M

Baum, M.J. & Cherry, J.A. (2015) Processing by the main olfactory system of chemosignals that facilitate mammalian reproduction. *Hormones and Behavior*, 68, 53–64. Available from: https://doi.org/10.1016/j.yhbeh.2014.06.003

Bednar, M. & Langfelder, O. (1930) Über das intravenose (hämatogene) riechen. *Monatsschrift für Ohrenheilkunde*, 64, 1133–1139.

Bergström, A., Stanton, D.W.G., Taron, U.H., Frantz, L., Sinding, M.H.S., Ersmark, E. et al. (2022) Grey wolf genomic history reveals a dual ancestry of dogs. *Nature*, 607(7918), 313–320. Available from: https://doi.org/10.1038/s41586-022-04824-9

Bhatnagar, K.P. & Meisami, E. (1998) Vomeronasal organ in bats and primates: extremes of structural variability and its phylogenetic implications. *Microscopy Research and Technique*, 43(6), 465–475. Available from: https://doi.org/10.1002/(SICI)1097-0029(19981215)43:6<465::AID-JEMT1>3.0.CO;2-1

Bhatnagar, K.P. & Smith, T.D. (2007) Light microscopic and ultrastructural observations on the vomeronasal organ of Anoura (Chiroptera: Phyllostomidae). *The Anatomical Record: Advances in Integrative Anatomy and Evolutionary Biology*, 290(11), 1341–1354. Available from: https://doi.org/10.1002/ar.20601

Bignami, A., Eng, L.F., Dahl, D. & Uyeda, C.T. (1972) Localization of the glial fibrillary acidic protein in astrocytes by immunofluorescence.

Brain Research, 43(2), 429–435. Available from: https://doi.org/10.1016/0006-8993(72)90398-8

Boillat, M., Challet, L., Rossier, D., Kan, C., Carleton, A. & Rodriguez, I. (2015) The vomeronasal system mediates sick conspecific avoidance. *Current Biology*, 25(2), 251–255. Available from: https://doi.org/10.1016/j.cub.2014.11.061

Breipohl, W., Bhatnagar, K.P., Blank, M. & Mendoza, A.S. (1981) Intraepithelial blood vessels in the vomeronasal neuroepithelium of the rat: a light and electron microscopic study. *Cell and Tissue Research*, 215(3), 465–473. Available from: https://doi.org/10.1007/BF00233523

Bressel, O.C., Khan, M. & Mombaerts, P. (2016) Linear correlation between the number of olfactory sensory neurons expressing a given mouse odorant receptor gene and the total volume of the corresponding glomeruli in the olfactory bulb: mouse olfactory sensory neurons. *Journal of Comparative Neurology*, 524(1), 199–209. Available from: https://doi.org/10.1002/cne.23835

Briñón, J.G., Weruaga, E., Crespo, C., Porteros, A., Arévalo, R., Aijón, J. et al. (2001) Calretinin-, neurocalcin-, and parvalbumin-immunoreactive elements in the olfactory bulb of the hedgehog (Erinaceus europaeus). *The Journal of Comparative Neurology*, 429(4), 554–570.

Bufe, B., Teuchert, Y., Schmid, A., Pyrski, M., Pérez-Gómez, A., Eisenbeis, J. et al. (2019) Bacterial MgrB peptide activates chemoreceptor Fpr3 in mouse accessory olfactory system and drives avoidance behaviour. *Nature Communications*, 10(1), 4889. Available from: https://doi.org/10.1038/s41467-019-12842-x

Chengetanai, S., Bhagwandin, A., Bertelsen, M.F., Hård, T., Hof, P.R., Spocter, M.A. et al. (2020) The brain of the African wild dog. II. The olfactory system. *Journal of Comparative Neurology*, 528(18), 3285–3304. Available from: https://doi.org/10.1002/cne.25007

Crespo, C., Alonso, J.R., Briñón, J.G., Weruaga, E., Porteros, A., Arévalo, R. et al. (1997) Calcium-binding proteins in the periglomerular region of typical and atypical olfactory glomeruli. *Brain Research*, 745(1–2), 293–302. Available from: https://doi.org/10.1016/S0006-8993(96)01185-7

de la Rosa-Prieto, C., Saiz-Sanchez, D., Ubeda-Bañon, I., Argandoña-Palacios, L., Garcia-Muñozguren, S. & Martinez-Marcos, A. (2010) Neurogenesis in subclasses of vomeronasal sensory neurons in adult mice. *Developmental Neurobiology*, 70(14), 961–970. Available from: https://doi.org/10.1002/dneu.20838

Dennis, J.C., Allgier, J.G., Desouza, L.S., Eward, W.C. & Morrison, E.E. (2003) Immunohistochemistry of the canine vomeronasal organ. *Journal of Anatomy*, 203(3), 329–338. Available from: https://doi.org/10.1046/j.1469-7580.2003.00190.x

Dennis, J.C., Stilwell, N.K., Smith, T.D., Park, T.J., Bhatnagar, K.P. & Morrison, E.E. (2020) Is the mole rat vomeronasal organ functional? *The Anatomical Record*, 303(2), 318–329. Available from: https://doi.org/10.1002/ar.24060

Dietschi, Q., Tuberosa, J., Fodoulian, L., Boillat, M., Kan, C., Codourey, J. et al. (2022) Clustering of vomeronasal receptor genes is required for transcriptional stability but not for choice. *Science Advances*, 8(46), eabn7450. Available from: https://doi.org/10.1126/sciadv.abn7450

Doucette, J.R., Kiernan, J.A. & Flumerfelt, B.A. (1983) The re-innervation of olfactory glomeruli following transection of primary olfactory axons in the central or peripheral nervous system. *Journal of Anatomy*, 137(Pt 1), 1–19.

Dulac, C. & Axel, R. (1995) A novel family of genes encoding putative pheromone receptors in mammals. *Cell*, 83(2), 195–206. Available from: https://doi.org/10.1016/0092-8674(95)90161-2

Dzięcioł, M., Podgórski, P., Stańczyk, E., Szumny, A., Woszczyło, M., Pieczewska, B. et al. (2020) MRI features of the vomeronasal organ in dogs (*Canis Familiaris*). *Frontiers in Veterinary Science*, 7, 159. Available from: https://doi.org/10.3389/fvets.2020.00159

Eccles, R. (1982) Autonomic innervation of the vomeronasal organ of the cat. *Physiology & Behavior*, 28(6), 1011–1015. Available from: https://doi.org/10.1016/0031-9384(82)90168-8

Farbman, A.I. & Margolis, F.L. (1980) Olfactory marker protein during ontogeny: immunohistochemical localization. *Developmental Biology*, 74(1), 205–215. Available from: https://doi.org/10.1016/0012-1606(80)90062-7

Fortes-Marco, L., Lanuza, E. & Martinez-Garcia, F. (2013) Of pheromones and kairomones: what receptors mediate innate emotional responses? Pheromones and kairomones. *The Anatomical Record*, 296(9), 1346–1363. Available from: https://doi.org/10.1002/ar.22745

Fortes-Marco, L., Lanuza, E., Martínez-García, F. & Agustín-Pavón, C. (2015) Avoidance and contextual learning induced by a kairomone, a pheromone and a common odorant in female CD1 mice. *Frontiers in Neuroscience*, 9, 336. Available from: https://doi.org/10.3389/fnins.2015.00336

Frahm, H.D. & Bhatnagar, K.P. (1980) Comparative morphology of the accessory olfactory bulb in bats. *Journal of Anatomy*, 130(Pt 2), 349–365.

Fritts, S.H., Paul, L.D., Mech, L.D. and Scott, D.P. 1992. *Trends and management of wolf-livestock conflicts in Minnesota*. Washington, DC: U.S. Fish and Wildlife Service

Gispen, W.H., Nielander, H.B., De Graan, P.N.E., Oestreicher, A.B., Schrama, L.H. & Schotman, P. (1991) Role of the growth-associated protein B-50/GAP-43 in neuronal plasticity. *Molecular Neurobiology*, 5(2–4), 61–85. Available from: https://doi.org/10.1007/BF02935540

Gorman, M.L. & Trowbridge, B.J. (1989) The role of odor in the social lives of carnivores. In: Gittleman, J.L. (Ed.) *Carnivore behavior, ecology, and evolution*. Springer US: Boston, MA, pp. 57–88. Available from: https://doi.org/10.1007/978-1-4757-4716-4_3 [Accessed: 2 September 2023].

Graphodatsky, A.S., Perelman, P.L., Sokolovskaya, N.V., Beklemisheva, V.R., Serdukova, N.A., Dobigny, G. et al. (2008) Phylogenomics of the dog and fox family (Canidae, carnivora) revealed by chromosome painting. *Chromosome Research*, 16(1), 129–143. Available from: https://doi.org/10.1007/s10577-007-1203-5

Gustavson, C.R. & Nicolaus, L.K. (1987) Taste aversion conditioning in wolves, coyotes and other canids: retrospect and prospect. In: Frank, H. (Ed.) *Man and wolf: Advances, issues, and problems in caplive wolf research*. Dordrecht, Netherlands: Dr. W. Junk Publishers, pp. 169–200.

Halpern, M. & Martínez-Marcos, A. (2003) Structure and function of the vomeronasal system: an update. *Progress in Neurobiology*, 70(3), 245–318. Available from: https://doi.org/10.1016/S0301-0082(03)00103-5

Halpern, M., Shapiro, L.S. & Jia, C. (1995) Differential localization of G proteins in the opossum vomeronasal system. *Brain Research*, 677(1), 157–161. Available from: https://doi.org/10.1016/0006-8993(95)00159-N

Hasui, K., Takatsuka, T., Sakamoto, R., Matsushita, S., Tsuyama, S., Izumo, S. et al. (2003) Double autoimmunostaining with glycine treatment. *The Journal of Histochemistry and Cytochemistry*, 51(9), 1169–1176. Available from: https://doi.org/10.1177/002215540305100907

Herrada, G. & Dulac, C. (1997) A novel family of putative pheromone receptors in mammals with a topographically organized and sexually dimorphic distribution. *Cell*, 90(4), 763–773. Available from: https://doi.org/10.1016/S0092-8674(00)80536-X

Ichikawa, M., Osada, T. & Ikai, A. (1992) Bandeiraea simplicifolia lectin I and Vicia villosa agglutinin bind specifically to the vomeronasal axons in the accessory olfactory bulb of the rat. *Neuroscience Research*, 13(1), 73–79. Available from: https://doi.org/10.1016/0168-0102(92)90035-B

Isogai, Y., Si, S., Pont-Lezica, L., Tan, T., Kapoor, V., Murthy, V.N. et al. (2011) Molecular organization of vomeronasal chemoreception. *Nature*, 478(7368), 241–245. Available from: https://doi.org/10.1038/nature10437

Iwanaga, T. & Nio-Kobayashi, J. (2020) Unique blood vasculature and innervation in the cavernous tissue of murine vomeronasal organs. *Biomedical Research*, 41(5), 243–251. Available from: https://doi.org/10.2220/biomedres.41.243

Jacobs, V.L., Sis, R.F., Chenoweth, P.J., Klemm, W.R. & Sherry, C.J. (1981) Structures of the bovine vomeronasal complex and its relationships to the palate: tongue manipulation. *Cells, Tissues, Organs*, 110(1), 48–58. Available from: https://doi.org/10.1159/000145412

Jawlowski, H. (1956) On the bulbus olfactorius and bulbus olfactorius accessorius of some mammals. *Lublin Uniwersytet Marii Curie-Sklodowskiej Roczniki. Annls Dzialc Nauki Biologiczne*, 10, 67–86.

Jezierski, T., Ensminger, J. & Papet, L.E. (2016) *Canine olfaction science and law: advances in forensic science, medicine.* S.L.: CRC Press.

Jia, C. & Halpern, M. (2004) Calbindin D28k, parvalbumin, and calretinin immunoreactivity in the main and accessory olfactory bulbs of the gray short-tailed opossum, Monodelphis domestica. *Journal of Morphology*, 259(3), 271–280. Available from: https://doi.org/10.1002/jmor.10166

Kelliher, K.R., Baum, M.J. & Meredith, M. (2001) The Ferret's vomeronasal organ and accessory olfactory bulb: effect of hormone manipulation in adult males and females. *The Anatomical Record*, 263(3), 280–288. Available from: https://doi.org/10.1002/ar.1097

Kohl, J., Autry, A.E. & Dulac, C. (2017) The neurobiology of parenting: a neural circuit perspective. *BioEssays*, 39(1), e201600159. Available from: https://doi.org/10.1002/bies.201600159

Kondoh, D., Tanaka, Y., Kawai, Y.K., Mineshige, T., Watanabe, K. & Kobayashi, Y. (2021) Morphological and histological features of the vomeronasal organ in African pygmy hedgehog (*Atelerix albiventris*). *Animals*, 11(5), 1462. Available from: https://doi.org/10.3390/ani11051462

Kondoh, D., Tomiyasu, J., Itakura, R., Sugahara, M., Yanagawa, M., Watanabe, K. et al. (2020) Comparative histological studies on properties of polysaccharides secreted by vomeronasal glands of eight Laurasiatheria species. *Acta Histochemica*, 122(3), 151515. Available from: https://doi.org/10.1016/j.acthis.2020.151515

Kratzing, J. (1971) The structure of the vomeronasal organ in the sheep. *Journal of Anatomy*, 108(Pt 2), 247–260.

Kunkhyen, T., McCarthy, E.A., Korzan, W.J., Doctor, D., Han, X., Baum, M.J. et al. (2017) Optogenetic activation of accessory olfactory bulb input to the forebrain differentially modulates investigation of opposite versus same-sex urinary Chemosignals and stimulates mating in male mice. *Eneuro*, 4(2), ENEURO.0010-17.2017. Available from: https://doi.org/10.1523/ENEURO.0010-17.2017

Leinders-Zufall, T., Ishii, T., Chamero, P., Hendrix, P., Oboti, L., Schmid, A. et al. (2014) A family of nonclassical class I MHC genes contributes to ultrasensitive chemodetection by mouse vomeronasal sensory neurons. *Journal of Neuroscience*, 34(15), 5121–5133. Available from: https://doi.org/10.1523/JNEUROSCI.0186-14.2014

Leinders-Zufall, T., Lane, A.P., Puche, A.C., Ma, W., Novotny, M.V., Shipley, M.T. et al. (2000) Ultrasensitive pheromone detection by mammalian vomeronasal neurons. *Nature*, 405(6788), 792–796. Available from: https://doi.org/10.1038/35015572

Levy, D.R., Sofer, Y., Brumfeld, V., Zilkha, N. & Kimchi, T. (2020) The nasopalatine ducts are required for proper pheromone signaling in mice. *Frontiers in Neuroscience*, 14, 585323. Available from: https://doi.org/10.3389/fnins.2020.585323

Loo, S.K. & Kanagasunteram, R. (1972) The vomeronasal organ in tree shrew and slow loris. *Journal of Anatomy*, 112(Pt 2), 165–172.

Macdonald, D.W., Campbell, L.A.D., Kamler, J.F., Marino, J., Werhahn, G. & Sillero-Zubiri, C. (2019) Monogamy: cause, consequence, or corollary of success in wild canids? *Frontiers in Ecology and Evolution*, 7, 341. Available from: https://doi.org/10.3389/fevo.2019.00341

Mahdy, E., behery, E. & Mohamed, S. (2019) Comparative morpho-histological analysis on the vomeronasal organ and the accessory olfactory bulb in Balady dogs (*Canis familiaris*) and New Zealand rabbits (*Oryctolagus cuniculus*). *Journal of Advanced Veterinary and Animal Research*, 6(4), 506–515. Available from: https://doi.org/10.5455/javar.2019.f375

Malz, C.R., Knabe, W. & Kuhn, H.-J. (2000) Pattern of calretinin immunoreactivity in the main olfactory system and the vomeronasal system of the tree shrew, *Tupaia belangeri*. *The Journal of Comparative Neurology*, 420(4), 428–436. Available from: https://doi.org/10.1002/(SICI)1096-9861(20000515)420:4<428::AID-CNE2>3.0.CO;2-2

Matsunami, H. & Buck, L.B. (1997) A multigene family encoding a diverse array of putative pheromone receptors in mammals. *Cell*, 90(4), 775–784. Available from: https://doi.org/10.1016/S0092-8674(00)80537-1

McCotter, R.E. (1912) The connection of the vomeronasal nerves with the accessory olfactory bulb in the opossum and other mammals. *The Anatomical Record*, 6(8), 299–318. Available from: https://doi.org/10.1002/ar.1090060802

Mech, L.D. (1995) The challenge and opportunity of recovering wolf populations. *Conservation Biology*, 9(2), 270–278. Available from: https://doi.org/10.1046/j.1523-1739.1995.9020270.x

Mechin, V., Pageat, P., Teruel, E. & Asproni, P. (2021) Histological and immunohistochemical characterization of vomeronasal organ aging in mice. *Animals*, 11(5), 1211. Available from: https://doi.org/10.3390/ani11051211

Meisami, E. & Bhatnagar, K.P. (1998) Structure and diversity in mammalian accessory olfactory bulb. *Microscopy Research and Technique*, 43(6), 476–499. Available from: https://doi.org/10.1002/(SICI)1097-0029(19981215)43:6<476::AID-JEMT2>3.0.CO;2-V

Meredith, M. (1994) Chronic recording of vomeronasal pump activation in awake behaving hamsters. *Physiology & Behavior*, 56(2), 345–354. Available from: https://doi.org/10.1016/0031-9384(94)90205-4

Meredith, M., Marques, D.M., O'Connell, R.J. & Stern, F.L. (1980) Vomeronasal pump: significance for male hamster sexual behavior. *Science*, 207(4436), 1224–1226. Available from: https://doi.org/10.1126/science.7355286

Meredith, M. & O'Connell, R.J. (1979) Efferent control of stimulus access to the hamster vomeronasal organ. *The Journal of Physiology*, 286(1), 301–316. Available from: https://doi.org/10.1113/jphysiol.1979.sp012620

Miodonski, R. (1968) Bulbus olfactorius of the dog (*Canis familiaris*). *Acta Biologica Cracoviensia*, 11, 65–76.

Moawad, U.K., Awaad, A.S. & Abedellaah, B.A. (2017) Morphological, histochemical and computed tomography on the vomeronasal organ (Jacobson's organ) of Egyptian native breeds of goats (Capra hircus). *Beni-Suef University Journal of Basic and Applied Sciences*, 6(2), 174–183. Available from: https://doi.org/10.1016/j.bjbas.2017.03.003

Mohrhardt, J., Nagel, M., Fleck, D., Ben-Shaul, Y. & Spehr, M. (2018) Signal detection and coding in the accessory olfactory system. *Chemical Senses*, 43(9), 667–695. Available from: https://doi.org/10.1093/chemse/bjy061

Mucignat, C. (2004) High-resolution magnetic resonance spectroscopy of the mouse vomeronasal organ. *Chemical Senses*, 29(8), 693–696. Available from: https://doi.org/10.1093/chemse/bjh073

Muñiz-de Miguel, S., Barreiro-Vázquez, J.D., Sánchez-Quinteiro, P., Ortiz-Leal, I. & González-Martínez, Á. (2023) Behavioural disorder in a dog with congenital agenesis of the vomeronasal organ and the septum pellucidum. *Veterinary Record Case Reports*, 11(2), e571. Available from: https://doi.org/10.1002/vrc2.571

Nakajima, T., Sakaue, M., Kato, M., Saito, S., Ogawa, K. & Taniguchi, K. (1998) Immunohistochemical and enzyme-histochemical study on

the accessory olfactory bulb of the dog. *The Anatomical Record*, 252(3), 393–402. Available from: https://doi.org/10.1002/(SICI)1097-0185(199811)252:3<393::AID-AR7>3.0.CO;2-T

Navarro-Moreno, C., Sanchez-Catalan, M.J., Barneo-Muñoz, M., Goterris-Cerisuelo, R., Belles, M., Lanuza, E. et al. (2020) Pregnancy changes the response of the vomeronasal and olfactory systems to pups in mice. *Frontiers in Cellular Neuroscience*, 14, 593309. Available from: https://doi.org/10.3389/fncel.2020.593309

Niven, J.E. & Laughlin, S.B. (2008) Energy limitation as a selective pressure on the evolution of sensory systems. *Journal of Experimental Biology*, 211(11), 1792–1804. Available from: https://doi.org/10.1242/jeb.017574

Oboti, L., Ibarra-Soria, X., Pérez-Gómez, A., Schmid, A., Pyrski, M., Paschek, N. et al. (2015) Pregnancy and estrogen enhance neural progenitor-cell proliferation in the vomeronasal sensory epithelium. *BMC Biology*, 13(1), 104. Available from: https://doi.org/10.1186/s12915-015-0211-8

Ogura, T., Krosnowski, K., Zhang, L., Bekkerman, M. & Lin, W. (2010) Chemoreception regulates chemical access to mouse vomeronasal organ: role of solitary chemosensory cells. Koch, K.-W. ed. *PLoS One*, 5(7), e11924. Available from: https://doi.org/10.1371/journal.pone.0011924

Ortiz-Hidalgo, C. (2011) Abelardo Gallego (1879–1930) and his contributions to histotechnology: the Gallego stains. *Acta Histochemica*, 113(2), 189–193. Available from: https://doi.org/10.1016/j.acthis.2009.09.010

Ortiz-Leal, I., Torres, M.V., López-Callejo, L.N., Fidalgo, L.E., López-Beceiro, A. & Sanchez-Quinteiro, P. (2022) Comparative neuroanatomical study of the main olfactory bulb in domestic and wild canids: dog, wolf and red fox. *Animals*, 12(9), 1079. Available from: https://doi.org/10.3390/ani12091079

Ortiz-Leal, I., Torres, M.V., Vargas-Barroso, V., Fidalgo, L.E., López-Beceiro, A.M., Larriva-Sahd, J.A. et al. (2023) The olfactory limbus of the red fox (Vulpes vulpes). New insights regarding a noncanonical olfactory bulb pathway. *Frontiers in Neuroanatomy*, 16, 1097467.

Ortiz-Leal, I., Torres, M.V., Villamayor, P.R., Fidalgo, L.E., López-Beceiro, A. & Sanchez-Quinteiro, P. (2022) Can domestication shape Canidae brain morphology? The accessory olfactory bulb of the red fox as a case in point. *Annals of Anatomy – Anatomischer Anzeiger*, 240, 151881. Available from: https://doi.org/10.1016/j.aanat.2021.151881

Ortiz-Leal, I., Torres, M.V., Villamayor, P.R., López-Beceiro, A. & Sanchez-Quinteiro, P. (2020) The vomeronasal organ of wild canids: the fox (*Vulpes vulpes*) as a model. *Journal of Anatomy*, 237(5), 890–906. Available from: https://doi.org/10.1111/joa.13254

Osakada, T., Abe, T., Itakura, T., Mori, H., Ishii, K.K., Eguchi, R. et al. (2022) Hemoglobin in the blood acts as a chemosensory signal via the mouse vomeronasal system. *Nature Communications*, 13(1), 556. Available from: https://doi.org/10.1038/s41467-022-28118-w

Pageat, P. & Gaultier, E. (2003) Current research in canine and feline pheromones. *Veterinary Clinics of North America: Small Animal Practice*, 33(2), 187–211. Available from: https://doi.org/10.1016/S0195-5616(02)00128-6

Peters, R.P. & Mech, L.D. (1975) Scent-marking in wolves. *American Scientist*, 63(6), 628–637.

Petrulis, A. (2013) Chemosignals, hormones and mammalian reproduction. *Hormones and Behavior*, 63(5), 723–741. Available from: https://doi.org/10.1016/j.yhbeh.2013.03.011

Powers, J.B. & Winans, S.S. (1975) Vomeronasal organ: critical role in mediating sexual behavior of the male hamster. *Science*, 187(4180), 961–963. Available from: https://doi.org/10.1126/science.1145182

Prieto-Godino, L.L., Rytz, R., Bargeton, B., Abuin, L., Arguello, J.R., Peraro, M.D. et al. (2016) Olfactory receptor pseudo-pseudogenes. *Nature*, 539(7627), 93–97. Available from: https://doi.org/10.1038/nature19824

Prince, J.E.A., Cho, J.H., Dumontier, E., Andrews, W., Cutforth, T., Tessier-Lavigne, M. et al. (2009) Robo-2 controls the segregation of a portion of basal vomeronasal sensory neuron axons to the posterior region of the accessory olfactory bulb. *Journal of Neuroscience*, 29(45), 14211–14222. Available from: https://doi.org/10.1523/JNEUROSCI.3948-09.2009

Ramakers, G.J.A., Verhaagen, J., Oestreicher, A.B., Margolis, F.L., Van Bergen En Henegouwen, P.M.P. & Gispen, W.H. (1992) Immunolocalization of B-50 (GAP-43) in the mouse olfactory bulb: predominant presence in preterminal axons. *Journal of Neurocytology*, 21(12), 853–869. Available from: https://doi.org/10.1007/BF01191683

Raymer, J., Wiesler, D., Novotny, M., Asa, C., Seal, U.S. & Mech, L.D. (1985) Chemical investigations of wolf (Canis lupus) anal-sac secretion in relation to breeding season. *Journal of Chemical Ecology*, 11(5), 593–608. Available from: https://doi.org/10.1007/BF00988570

Raymer, J., Wiesler, D., Novotny, M., Asa, C., Seal, U.S. & Mech, L.D. (1986) Chemical scent constituents in urine of wolf (Canis lupus) and their dependence on reproductive hormones. *Journal of Chemical Ecology*, 12(1), 297–314. Available from: https://doi.org/10.1007/BF01045612

Riddell, P., Paris, M.C.J., Joonè, C.J., Pageat, P. & Paris, D.B.B.P. (2021) Appeasing pheromones for the management of stress and aggression during conservation of wild canids: could the solution be right under our nose? *Animals*, 11(6), 1574. Available from: https://doi.org/10.3390/ani11061574

Rodewald, A., Gisder, D., Gebhart, V.M., Oehring, H. & Jirikowski, G.F. (2016) Distribution of olfactory marker protein in the rat vomeronasal organ. *Journal of Chemical Neuroanatomy*, 77, 19–23. Available from: https://doi.org/10.1016/j.jchemneu.2016.04.002

Rothman, R.J. & Mech, L.D. (1979) Scent-marking in lone wolves and newly formed pairs. *Animal Behaviour*, 27, 750–760. Available from: https://doi.org/10.1016/0003-3472(79)90010-1

Równiak, M. & Bogus-Nowakowska, K. (2020) The amygdala of the common shrew, Guinea pig, rabbit, fox and pig: five flavours of the mammalian amygdala as a consequence of clade-specific mosaic-like evolution. *Journal of Anatomy*, 236(5), 891–905. Available from: https://doi.org/10.1111/joa.13148

Równiak, M., Bogus-Nowakowska, K., Kalinowski, D. & Kozłowska, A. (2022) The evolutionary trajectories of the individual amygdala nuclei in the common shrew, Guinea pig, rabbit, fox and pig: a consequence of embryological fate and mosaic-like evolution. *Journal of Anatomy*, 240(3), 489–502. Available from: https://doi.org/10.1111/joa.13571

Ryba, N.J.P. & Tirindelli, R. (1997) A new multigene family of putative pheromone receptors. *Neuron*, 19(2), 371–379. Available from: https://doi.org/10.1016/S0896-6273(00)80946-0

Salazar, I., Barber, P.C. & Cifuentes, J.M. (1992) Anatomical and immunohistological demonstration of the primary neural connections of the vomeronasal organ in the dog. *The Anatomical Record*, 233(2), 309–313. Available from: https://doi.org/10.1002/ar.1092330214

Salazar, I., Cifuentes, J.M., Quinteiro, P.S. & Caballero, G. (1994) The vomeronasal system of the mink, *Mustela vison*. I. The vomeronasal organ. *Functional and Developmental Morphology*, 4(2), 113–117.

Salazar, I., Cifuentes, J.M., Sánchez Quinteiro, P. & García Caballero, T. (1994) Structural, morphometric, and immunohistological study of the accessory olfactory bulb in the dog. *The Anatomical Record*, 240(2), 277–285. Available from: https://doi.org/10.1002/ar.1092400216

Salazar, I., Cifuentes, J.M. & Sánchez-Quinteiro, P. (2013) Morphological and immunohistochemical features of the vomeronasal system in dogs. *The Anatomical Record: Advances in Integrative Anatomy and Evolutionary Biology*, 296(1), 146–155. Available from: https://doi.org/10.1002/ar.22617

Salazar, I., Lombardero, M., Cifuentes, J.M., Quinteiro, P.S. & Aleman, N. (2003) Morphogenesis and growth of the soft tissue and cartilage of

the vomeronasal organ in pigs. *Journal of Anatomy*, 202(6), 503–514. Available from: https://doi.org/10.1046/j.1469-7580.2003.00183.x

Salazar, I., Quinteiro, P.S., Alemañ, N., Cifuentes, J.M. & Troconiz, P.F. (2007) Diversity of the vomeronasal system in mammals: the singularities of the sheep model. *Microscopy Research and Technique*, 70(8), 752–762. Available from: https://doi.org/10.1002/jemt.20461

Salazar, I., Quinteiro, P.S. & Cifuentes, J.M. (1995) Comparative anatomy of the vomeronasal cartilage in mammals: mink, cat, dog, pig, cow and horse. *Annals of Anatomy - Anatomischer Anzeiger*, 177(5), 475–481. Available from: https://doi.org/10.1016/S0940-9602(11)80156-1

Salazar, I., Quinteiro, P.S., Cifuentes, J.M. & Lombardero, M. (1998) The accessory olfactory bulb of the mink, Mustela vison: a morphological and lectin histochemical study. *Anatomia, Histologia, Embryologia: Journal of Veterinary Medicine Series C*, 27(5), 297–300. Available from: https://doi.org/10.1111/j.1439-0264.1998.tb00197.x

Salazar, I., Sánchez Quinteiro, P., Cifuentes, J.M., Fernández, P. & Lombardero, M. (1997) Distribution of the arterial supply to the vomeronasal organ in the cat. *The Anatomical Record*, 247(1), 129–136. Available from: https://doi.org/10.1002/(SICI)1097-0185(199701)247:1<129::AID-AR15>3.0.CO;2-R

Salazar, I., Sanchez Quinteiro, P., Cifuentes, J.M. & Garcia Caballero, T. (1996) The vomeronasal organ of the cat. *Journal of Anatomy*, 188(Pt 2), 445–454.

Salazar, I. & Sánchez-Quinteiro, P. (2009) The risk of extrapolation in neuroanatomy: the case of the mammalian accessory olfactory bulb. *Frontiers in Neuroanatomy*, 3, 22. Available from: https://doi.org/10.3389/neuro.05.022.2009

Salazar, I. & Sánchez-Quinteiro, P. (2011) A detailed morphological study of the vomeronasal organ and the accessory olfactory bulb of cats. *Microscopy Research and Technique*, 74(12), 1109–1120. Available from: https://doi.org/10.1002/jemt.21002

Shinohara, H., Asano, T. & Kato, K. (1992) Differential localization of G-proteins Gi and Go in the accessory olfactory bulb of the rat. *The Journal of Neuroscience*, 12(4), 1275–1279. Available from: https://doi.org/10.1523/JNEUROSCI.12-04-01275.1992

Slotnick, B. (2001) Animal cognition and the rat olfactory system. *Trends in Cognitive Sciences*, 5(5), 216–222. Available from: https://doi.org/10.1016/S1364-6613(00)01625-9

Smith, T.D., Alport, L.J., Burrows, A.M., Bhatnagar, K.P., Dennis, J.C., Tuladhar, P. et al. (2007) Perinatal size and maturation of the olfactory and vomeronasal neuroepithelia in lorisoids and lemuroids. *American Journal of Primatology*, 69(1), 74–85. Available from: https://doi.org/10.1002/ajp.20328

Smith, T.D., Dennis, J.C., Bhatnagar, K.P., Garrett, E.C., Bonar, C.J. & Morrison, E.E. (2011) Olfactory marker protein expression in the vomeronasal neuroepithelium of tamarins (*Saguinus* spp). *Brain Research*, 1375, 7–18. Available from: https://doi.org/10.1016/j.brainres.2010.12.069

Smith, T.D., Garrett, E.C., Bhatnagar, K.P., Bonar, C.J., Bruening, A.E., Dennis, J.C. et al. (2011) The vomeronasal organ of New World monkeys (Platyrrhini). *The Anatomical Record: Advances in Integrative Anatomy and Evolutionary Biology*, 294(12), 2158–2178. Available from: https://doi.org/10.1002/ar.21509

Smith, T.D., Muchlinski, M.N., Bhatnagar, K.P., Durham, E.L., Bonar, C.J. & Burrows, A.M. (2015) The vomeronasal organ of *Lemur catta*: Lemur catta VNO. *American Journal of Primatology*, 77(2), 229–238. Available from: https://doi.org/10.1002/ajp.22326

Stensmyr, M.C. (2016) Evolutionary genetics: smells like a pseudopseudogene. *Current Biology*, 26(24), R1294–R1296. Available from: https://doi.org/10.1016/j.cub.2016.11.006

Stohr, C. & Coimbra, E. (2013) The governance of the wolf-human relationship in Europe. *Review of European Studies*, 5(4), p1. Available from: https://doi.org/10.5539/res.v5n4p1

Su, C.-Y., Menuz, K. & Carlson, J.R. (2009) Olfactory perception: receptors, cells, and circuits. *Cell*, 139(1), 45–59. Available from: https://doi.org/10.1016/j.cell.2009.09.015

Suárez, R., Fernández-Aburto, P., Manger, P.R. & Mpodozis, J. (2011) Deterioration of the Gαo vomeronasal pathway in sexually dimorphic mammals. Callaerts, P. ed. *PLoS One*, 6(10), e26436. Available from: https://doi.org/10.1371/journal.pone.0026436

Suárez, R. & Mpodozis, J. (2009) Heterogeneities of size and sexual dimorphism between the subdomains of the lateral-innervated accessory olfactory bulb (AOB) of *Octodon degus* (Rodentia: Hystricognathi). *Behavioural Brain Research*, 198(2), 306–312. Available from: https://doi.org/10.1016/j.bbr.2008.11.009

Suárez, R., Santibáñez, R., Parra, D., Coppi, A.A., Abrahão, L.M.B., Sasahara, T.H.C. et al. (2011) Shared and differential traits in the accessory olfactory bulb of caviomorph rodents with particular reference to the semiaquatic capybara: the AOB of capybaras and other caviomorphs. *Journal of Anatomy*, 218(5), 558–565. Available from: https://doi.org/10.1111/j.1469-7580.2011.01357.x

Suárez, R., Villalón, A., Künzle, H. & Mpodozis, J. (2009) Transposition and intermingling of Gαi2 and Gαo afferences into single vomeronasal glomeruli in the Madagascan lesser tenrec *Echinops telfairi*. Iwaniuk, A. ed. *PLoS One*, 4(11), e8005. Available from: https://doi.org/10.1371/journal.pone.0008005

Takami, S. (2002) Recent progress in the neurobiology of the vomeronasal organ. *Microscopy Research and Technique*, 58(3), 228–250. Available from: https://doi.org/10.1002/jemt.10094

Takigami, S. (2004) Morphological evidence for two types of mammalian vomeronasal system. *Chemical Senses*, 29(4), 301–310. Available from: https://doi.org/10.1093/chemse/bjh032

Takigami, S., Mori, Y. & Ichikawa, M. (2000) Projection pattern of vomeronasal neurons to the accessory olfactory bulb in goats. *Chemical Senses*, 25(4), 387–393. Available from: https://doi.org/10.1093/chemse/25.4.387

Tomiyasu, J., Kondoh, D., Sakamoto, H., Matsumoto, N., Haneda, S. & Matsui, M. (2018) Lectin histochemical studies on the olfactory gland and two types of gland in vomeronasal organ of the brown bear. *Acta Histochemica*, 120(6), 566–571. Available from: https://doi.org/10.1016/j.acthis.2018.07.003

Tomiyasu, J., Kondoh, D., Sakamoto, H., Matsumoto, N., Sasaki, M., Kitamura, N. et al. (2017) Morphological and histological features of the vomeronasal organ in the brown bear. *Journal of Anatomy*, 231(5), 749–757. Available from: https://doi.org/10.1111/joa.12673

Tomiyasu, J., Korzekwa, A., Kawai, Y.K., Robstad, C.A., Rosell, F. & Kondoh, D. (2022) The vomeronasal system in semiaquatic beavers. *Journal of Anatomy*, 241(3), 809–819. Available from: https://doi.org/10.1111/joa.13671

Torres, M.V., Ortiz-Leal, I., Ferreiro, A., Rois, J.L. & Sanchez-Quinteiro, P. (2021) Neuroanatomical and Immunohistological study of the Main and accessory olfactory bulbs of the meerkat (*Suricata suricatta*). *Animals*, 12(1), 91. Available from: https://doi.org/10.3390/ani12010091

Torres, M.V., Ortiz-Leal, I., Ferreiro, A., Rois, J.L. & Sanchez-Quinteiro, P. (2023) Immunohistological study of the unexplored vomeronasal organ of an endangered mammal, the dama gazelle (*Nanger dama*). *Microscopy Research and Technique*, 86(9), 1206–1233. Available from: https://doi.org/10.1002/jemt.24392

Torres, M.V., Ortiz-Leal, I. & Sanchez-Quinteiro, P. (2023) Pheromone sensing in mammals: a review of the vomeronasal system. *Anatomia*, 2(4), 346–413. Available from: https://doi.org/10.3390/anatomia2040031

Torres, M.V., Ortiz-Leal, I., Villamayor, P.R., Ferreiro, A., Rois, J.L. & Sanchez-Quinteiro, P. (2020) The vomeronasal system of the newborn capybara: a morphological and immunohistochemical study. *Scientific Reports*, 10(1), 13304. Available from: https://doi.org/10.1038/s41598-020-69994-w

Torres, M.V., Ortiz-Leal, I., Villamayor, P.R., Ferreiro, A., Rois, J.L. & Sanchez-Quinteiro, P. (2022) Does a third intermediate model for the vomeronasal processing of information exist? Insights from the macropodid neuroanatomy. *Brain Structure and Function*, 227(3), 881–899. Available from: https://doi.org/10.1007/s00429-021-02425-2

Tran, H., Chen, H., Walz, A., Posthumus, J.C. & Gong, Q. (2008) Influence of olfactory epithelium on mitral/tufted cell dendritic outgrowth. Hendricks, M. ed. *PLoS One*, 3(11), e3816. Available from: https://doi.org/10.1371/journal.pone.0003816

Tsunoda, M., Miyamichi, K., Eguchi, R., Sakuma, Y., Yoshihara, Y., Kikusui, T. et al. (2018) Identification of an intra- and inter-specific tear protein signal in rodents. *Current Biology*, 28(8), 1213–1223.e6. Available from: https://doi.org/10.1016/j.cub.2018.02.060

Ubeda-Bañon, I., Pro-Sistiaga, P., Mohedano-Moriano, A., Saiz-Sanchez, D., de la Rosa-Prieto, C., Gutierrez-Castellanos, N. et al. (2011) Cladistic analysis of olfactory and vomeronasal systems. *Frontiers in Neuroanatomy*, 5, 3. Available from: https://doi.org/10.3389/fnana.2011.00003

Vaccarezza, O.L., Sepich, L.N. & Tramezzani, J.H. (1981) The vomeronasal organ of the rat. *Journal of Anatomy*, 132(Pt 2), 167–185.

Van Den Berghe, F., Paris, M.C., Sarnyai, Z., Vlamings, B., Millar, R.P., Ganswindt, A. et al. (2019) Dog appeasing pheromone prevents the androgen surge and may reduce contact dominance and active submission after stressful interventions in African wild dogs (*Lycaon pictus*). Umapathy, G. ed. *PLoS One*, 14(3), e0212551. Available from: https://doi.org/10.1371/journal.pone.0212551

Vedin, V., Eriksson, B. & Berghard, A. (2010) Organization of the chemosensory neuroepithelium of the vomeronasal organ of the Scandinavian moose *Alces alces*. *Brain Research*, 1306, 53–61. Available from: https://doi.org/10.1016/j.brainres.2009.10.012

Verhaagen, J., Oestreicher, A., Gispen, W. & Margolis, F. (1989) The expression of the growth associated protein B50/GAP43 in the olfactory system of neonatal and adult rats. *The Journal of Neuroscience*, 9(2), 683–691. Available from: https://doi.org/10.1523/JNEUROSCI.09-02-00683.1989

Verhaagen, J., Oestreicher, A.B., Grillo, M., Khew-Goodall, Y.-S., Gispen, W.H. & Margolis, F.L. (1990) Neuroplasticity in the olfactory system: Differential effects of central and peripheral lesions of the primary olfactory pathway on the expression of B-50/GAP43 and the olfactory marker protein. *Journal of Neuroscience Research*, 26(1), 31–44. Available from: https://doi.org/10.1002/jnr.490260105

Villamayor, P.R., Arana, Á.J., Coppel, C., Ortiz-Leal, I., Torres, M.V., Sanchez-Quinteiro, P. et al. (2021) A comprehensive structural, lectin and immunohistochemical characterization of the zebrafish olfactory system. *Scientific Reports*, 11(1), 8865. Available from: https://doi.org/10.1038/s41598-021-88317-1

Villamayor, P.R., Cifuentes, J.M., Fdz.-de-Troconiz, P. & Sanchez-Quinteiro, P. (2018) Morphological and immunohistochemical study of the rabbit vomeronasal organ. *Journal of Anatomy*, 233(6), 814–827. Available from: https://doi.org/10.1111/joa.12884

Villamayor, P.R., Cifuentes, J.M., Quintela, L., Barcia, R. & Sanchez-Quinteiro, P. (2020) Structural, morphometric and immunohistochemical study of the rabbit accessory olfactory bulb. *Brain Structure and Function*, 225(1), 203–226. Available from: https://doi.org/10.1007/s00429-019-01997-4

Wielgus, R.B. & Peebles, K.A. (2014) Effects of wolf mortality on livestock depredations. Bump, J. K. ed. *PLoS One*, 9(12), e113505. Available from: https://doi.org/10.1371/journal.pone.0113505

Wirobski, G., Range, F., Schaebs, F.S., Palme, R., Deschner, T. & Marshall-Pescini, S. (2021) Endocrine changes related to dog domestication: Comparing urinary cortisol and oxytocin in hand-raised, pack-living dogs and wolves. *Hormones and Behavior*, 128, 104901. Available from: https://doi.org/10.1016/j.yhbeh.2020.104901

Yohe, L.R., Hoffmann, S. & Curtis, A. (2018) Vomeronasal and olfactory structures in bats revealed by DiceCT clarify genetic evidence of function. *Frontiers in Neuroanatomy*, 12, 32. Available from: https://doi.org/10.3389/fnana.2018.00032

Yohe, L.R. & Krell, N.T. (2023) An updated synthesis of and outstanding questions in the olfactory and vomeronasal systems in bats: genetics asks questions only anatomy can answer. *The Anatomical Record*, 306, 2765–2780. Available from: https://doi.org/10.1002/ar.25290

Young, J.M. & Trask, B.J. (2007) V2R gene families degenerated in primates, dog and cow, but expanded in opossum. *Trends in Genetics*, 23(5), 212–215. Available from: https://doi.org/10.1016/j.tig.2007.03.004

SUPPORTING INFORMATION

Additional supporting information can be found online in the Supporting Information section at the end of this article.